Low-spin structure of $^{86}_{35}Br_{51}$ and $^{86}_{36}Kr_{50}$ nuclei: The role of the $g_{7/2}$ neutron orbital

W. Urban,[1] K. Sieja,[2] T. Materna,[3] M. Czerwiński,[1] T. Rząca-Urban,[1] A. Blanc,[4] M. Jentschel,[4] P. Mutti,[4] U. Köster,[4] T. Soldner,[4] G. de France,[5] G. S. Simpson,[6,7] C. A. Ur,[8] C. Bernards,[9] C. Fransen,[9] J. Jolie,[9] J.-M. Regis,[9] T. Thomas,[9] and N. Warr[9]

[1]*Faculty of Physics, University of Warsaw, ul.Pasteura 5, PL-02-093 Warsaw, Poland*
[2]*Université de Strasbourg, IPHC, Strasbourg, France and CNRS, UMR7178, F-67037 Strasbourg, France*
[3]*CEA, DSM-Saclay, IRFU/SPhN, F-91191 Gif-sur-Yvette, France*
[4]*Institut Laue-Langevin, 71 Av. des Martyrs, F-38042 Grenoble Cedex, France*
[5]*Grand Accélérateur National d'Ions Lourds (GANIL), CEA/DSM – CNRS/IN2P3, Bd Henri Becquerel, BP 55027, F-14076 Caen Cedex 5, France*
[6]*LPSC, Université Joseph Fourier Grenoble 1, CNRS/IN2P3, Institut National Polytechnique de Grenoble, F-38026 Grenoble Cedex, France*
[7]*University of the West of Scotland, Paisley, PA1 2BE, United Kingdom*
[8]*INFN, I-35020 Legnaro, Italy*
[9]*IKP, Uniersität zu Köln, Zülpicherstr. 77, D-50937 Köln, Germany*

(Received 29 June 2016; published 28 October 2016)

Low-spin excited levels in $^{86}_{35}Br_{51}$ and $^{86}_{36}Kr_{50}$, populated following β^- decay and the neutron-induced fission of ^{235}U, were measured using the Lohengrin fission-fragment separator and the EXILL array of Ge detectors at the PF1B cold-neutron facility of the Institute Laue-Langevin Grenoble. Improved populations of excited levels in ^{86}Br remove inconsistencies existing in the literature on this nucleus. Directional-linear-polarization correlations, analyzed using newly developed formulas, as well as precise angular correlations allowed the unique 1^- and 2^- spin and parity assignments to the ground state of ^{86}Br and the 4016.3-keV level in ^{86}Kr, respectively. Based on these results we propose that the Gamow-Teller β^- decays of ^{86}Se and ^{86}Br involve the $\nu g_{7/2} \rightarrow \pi g_{9/2}$ transition in addition to the $\nu p_{3/2} \rightarrow \pi p_{3/2}$ transition proposed earlier. In ^{86}Kr we have identified 1^+_1, 2^+_3, and 3^+_1 levels, analogous to the mixed-symmetry states in ^{94}Mo, which in ^{86}Kr are from proton excitations, only. Large-scale, shell-model calculations with refined interactions reproduce well excitations in ^{86}Br and ^{86}Kr and support our interpretations.

DOI: 10.1103/PhysRevC.94.044328

I. INTRODUCTION

Recent studies of neutron-rich Se, Br, and Rb nuclei [1–8] provided valuable, new information on single-particle energies and couplings of protons and neutrons outside the ^{78}Ni core. However, as pointed out in the compilation [9], there are essential differences between the new picture and earlier β-decay works [10,11]. This is illustrated in Fig. 1, showing excited levels in ^{86}Br, with spins and parities as proposed in fusion-fission study [1]. The key, 7^+ spin and parity of the 1625.4-keV level in ^{86}Br [1] implies spin $I \geqslant 4$ for the 130.9-keV level and spin $I \geqslant 3$ for the 53.1-keV level. Both levels are assigned negative parity, natural for the $(\pi p^{-1}_{3/2} \nu d_{5/2})_j$ and $(\pi f^{-1}_{5/2} \nu d_{5/2})_j$ multiplets expected in ^{86}Br at low excitations [1]. The problem is the 12% feeding of the 53.1-keV level in β^- decay of the 0^+ ground state of ^{86}Se [11], which contradicts its 3^- spin and parity proposed in Ref. [1].

One may propose spin 2^- for the 53.1-keV level, shown as "alternative spins" at the right-hand side of Fig. 1. Then the spin of the ground state has to be lowered to 0^-. However, this is inconsistent with the β^- decay of ^{86}Br, which feeds the 4^+ level in ^{86}Kr [9]. To overcome this, one may further propose an extra β^- decay of the 4.4-keV, 2^- level in ^{86}Br, explaining at the same time the, to date not verified, low-energy $T_{1/2} \sim 5$ s isomer in ^{86}Br [11], which may be of importance for modeling processes in nuclear reactors. At present the production of $^{86}Br^m$ with $T_{1/2} = 4.5$ s in the $^{235}U + n_{th}$ fission is reported at the same level as that of the ground state of ^{86}Br [12].

The 2^- spin assignment to the 53.1-keV level forces lowering the spin of the 130.9-keV level to 3^- because of the prompt, dipole character of the 77.8-keV transition [1]. Consequently, the spin of the 1625.4-keV level has to be lowered to 6^+, because of the prompt character of the 1494.5-keV transition. This, however, disables the interpretation of this level as the $(\nu d_{5/2}, \pi g_{9/2})_{7^+}$, maximum aligned configuration, which is the key part of the picture proposed in Refs. [1,5,6].

Finally, there is a question about the Gamow-Teller β^- decay and the role of $g_{7/2}$ neutrons in the region. Despite numerous attempts [13–18] there is no consistent description of this important process, which decides about the ground-state half-lives of even-even nuclei in this region.

It is clear that a careful check of properties of ^{86}Br and ^{86}Kr is in order. In this work we have undertaken experimental studies of low-spin levels in ^{86}Br and ^{86}Kr, focusing on the verification of both spin assignments and β feedings to levels in both nuclei. We have also performed large-scale, shell-model calculations to understand excited levels in both nuclei. The experiment, data analysis, and results for both nuclei are described in Sec. II. In Sec. III the results are interpreted and compared to the shell-model calculations. The work is concluded in Sec. IV.

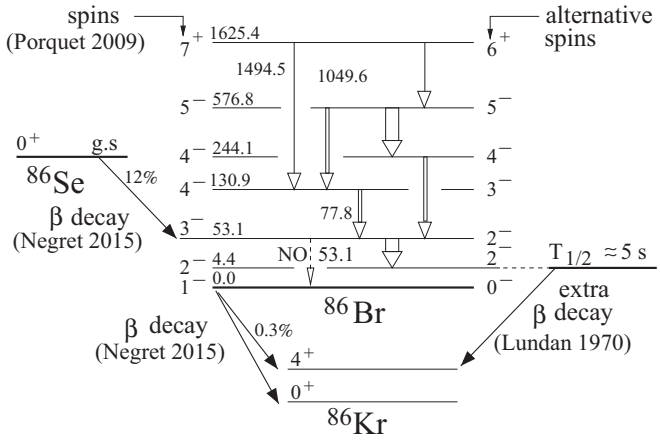

FIG. 1. Schematic, partial excitation scheme of ^{86}Br, drawn after Ref. [1]. Energies of γ lines and levels are given in keV. Thickness of arrows is proportional to the observed branching ratios. (Porquet 2009) [1], (Negret 2015) [9], (Lundan 1970) [11]. See text for further explanation.

II. EXPERIMENTS AND DATA ANALYSIS

Excited levels in ^{86}Br and ^{86}Kr, populated in β^- decay of ^{86}Se and ^{86}Br, respectively, have been studied using the Lohengrin fission-fragment separator [19,20] and an array of Ge detectors at the Institut Laue-Langevin (ILL), Grenoble. The experimental setup was described in our study of β^- decay of ^{86}As [7]. The independent yields for $A = 86$ isobars in the ^{235}U $+n_{th}$ fission are 0.02% for ^{86}As, 0.83% for ^{86}Se, 0.23% for ^{86}Br, and 0.23% for ^{86}Br^m [12], while the cumulative yields are 0.04% for ^{86}As, 1.2% for ^{86}Se, and 1.8% ^{86}Br [21]. It was possible to discriminate between the activities of various isobars because of different β-decay half-lives of ground states of the ^{86}As, ^{86}Se, and ^{86}Br mother nuclei, which are 0.9 s, 14.1 s, and 55.1 s, respectively. We used the electrostatic deflector of Lohengrin to create the time structure of the beam and the tape transport for periodical removal of activities from the measurement point. The tape cycle of 18 s comprised two subsequent deflector cycles (4 s beam-ON, 4 s beam-OFF) and 2 s for the tape movement, as shown schematically in Fig. 2.

In Figs. 2(a)–2(c) examples of time spectra gated on known lines of 704.3-keV in ^{86}Se, 48.7-keV in ^{86}Br, and 1564.7-keV in ^{86}Kr are shown. For the β^- decay of ^{86}As a complete activity growth and decay cycle is seen. In Fig. 2(b) corresponding to β^- decay of ^{86}Se this cycle are still pronounced. In case of β^- decay of ^{86}Br, shown in Fig. 2(c), the activity grows over the whole tape cycle, with only small influence from the beam ON and OFF cycles. This observation excludes any strong production of a hypothetical ^{86}Br^m with $T_{1/2} = 4.5$ s in the neutron-induced fission of ^{235}U, reported in Ref. [12].

In addition we used the data from the measurement of neutron-induced fission of ^{235}U using the EXILL Ge array [22,23], performed at the PF1B cold-neutron-beam facility [24] of the ILL. Detailed description of the experiment and the data-analysis technique is given in our recent works [5,6]. In the present work we analyzed prompt-γ decays of levels in ^{86}Br populated in fission and, in addition, decays of levels

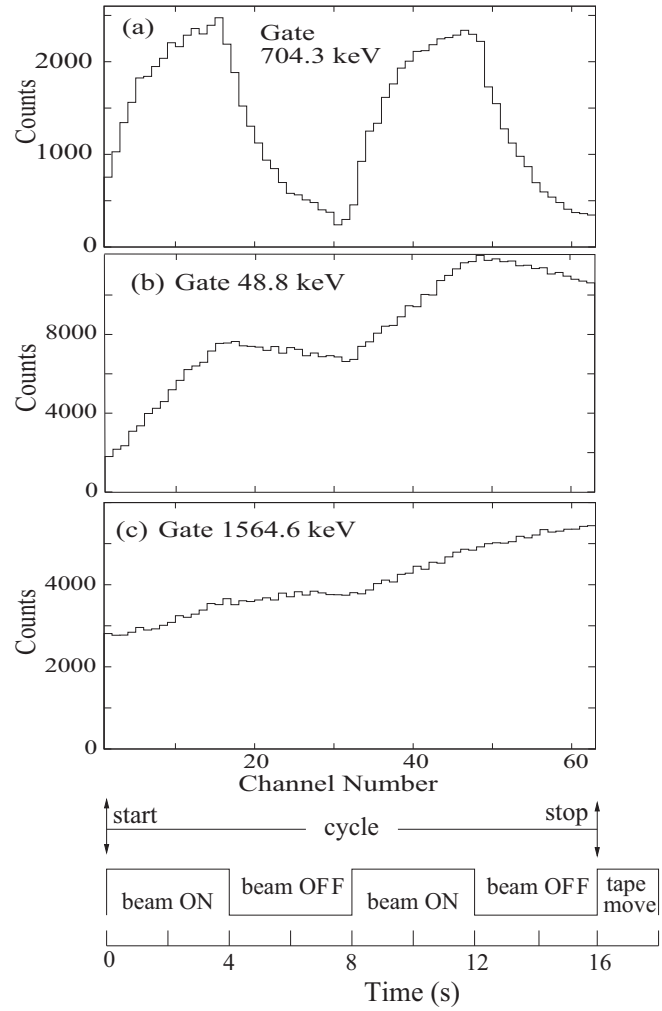

FIG. 2. Time spectra gated on the 704.3-keV line of ^{86}Se, the 48.7-keV line of ^{86}Br, and the 1564.7-keV line of ^{86}Kr. See text for more comments.

in ^{86}Kr, populated in β^- decay of ^{86}Br. The latter was particularly useful for studying angular correlations and linear polarization, utilizing the high symmetry of the EXILL array and the Clover symmetry of EXOGAM detectors [5,23,25].

A. Excited levels in ^{86}Br from β^- decay of ^{86}Se

The nucleus ^{86}Br was studied previously in β^- decay of ^{86}Se [10] where the (3^-) ground state and nine excited levels were proposed, including 1^+ levels at 2447.0 and 2665.1 keV, strongly populated in β^- decay. An earlier work [11] proposed in ^{86}Br a low-energy, 5-s isomer.

The scheme of excited states, populated in β^- decay of ^{86}Se, as obtained in this work is shown in Fig. 3. In Tables I and II properties of excited levels in ^{86}Br and their γ decays are presented. Relative γ-decay intensities, I_γ(rel.), are normalized to 100 for the 2442.5-keV line.

We confirm the 4.4-, 53.1-, 207.0-, 297.9-, 435.2-, 1047.3-2447.0-, and 2665.4-keV levels reported previously [9,10]). The 2661.0-keV decay of the 2665.4-keV level is now firmly established. To the decay branches of the 2447.0- and

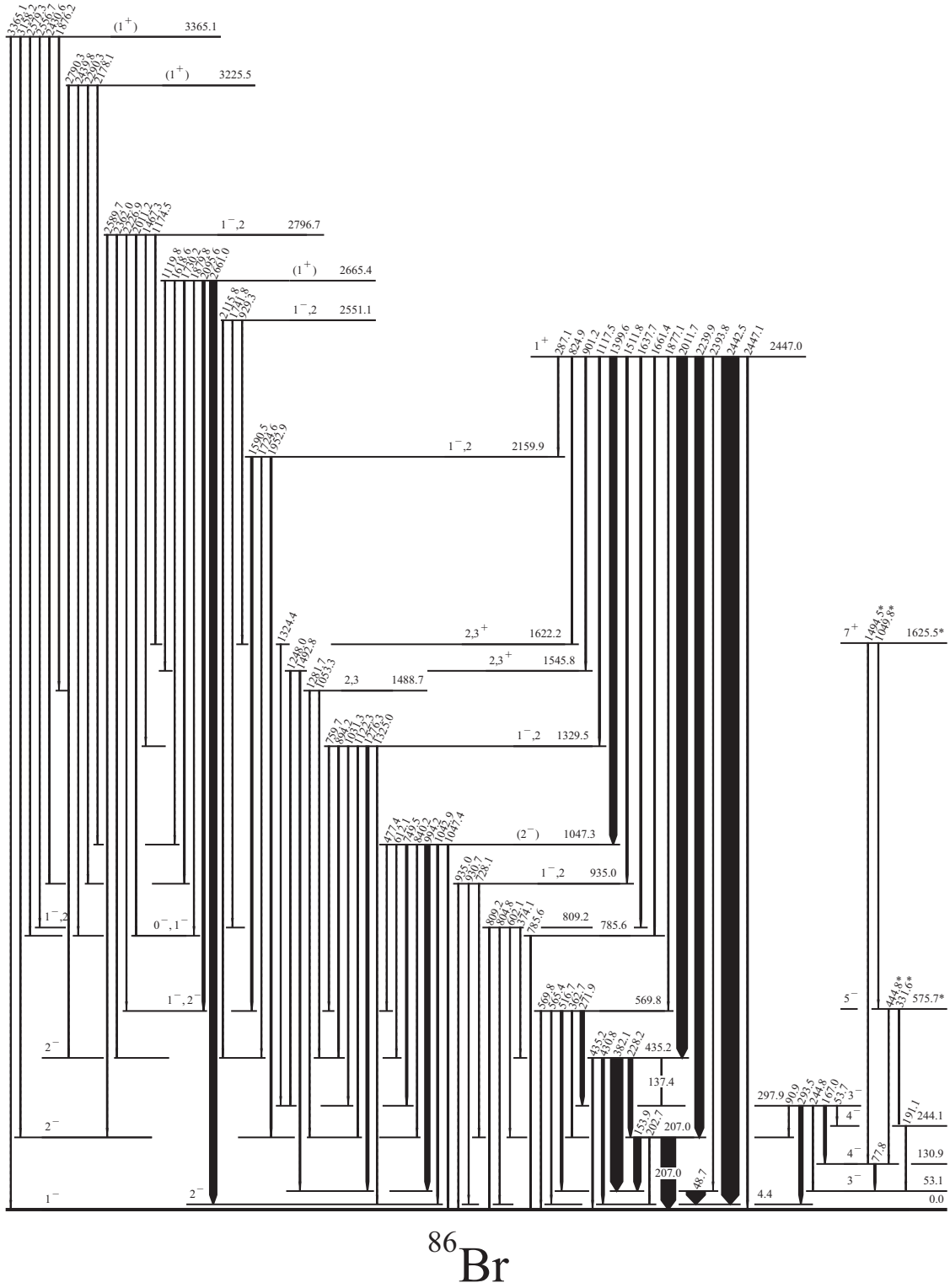

FIG. 3. Level scheme of ^{86}Br populated in β^- decay of ^{86}Se, as obtained in the present work. Energies of levels and γ decays are given in keV. Levels and transitions marked with an asterisk were populated in neutron-induced fission of ^{235}U, measured in the present work. See Tables I–III for more information on excited levels and their decays.

2665.4-keV, 1^+ levels we add new 287.1-, 824.9-, 901.2-, 1117.5-, 1877.1-, and 2447.1-keV and the 1119.8-, 1618.6-, 1730.2-, 1879.8-, and 2095.6-keV transitions, respectively. The new, 1117.5-keV decay of the 2446.8-keV level is introduced instead of the 1276.3-keV one by reversing the order of the 1117.0- and 1275.8-keV transitions reported in Ref. [9]. This defines a new level at 1329.5 keV, which replaces the 1170.4-keV level reported in Ref. [9]. The 1329.5-keV

TABLE I. Levels and their γ decays in ^{86}Br, as observed in β^- decay of ^{86}Se in the present work. See text for comments.

Level I^π	Level E_{exc} (keV)	γ decay E_γ (keV)	γ decay I_γ (rel.)	Level $P/100$	Level $\log_{10} ft$
1^-	0.0			39(4)	5.7(1)
2^-	4.40(5)			Assum. 2(2)	
3^-	53.12(5)	48.71(5)	79.0(60)	0.2(24)	
4^-	130.92(5)	77.80(5)	6.6(4)	0.0(4)	
2^-	207.03(5)	153.91(5)	27.7(9)	1.2(6)	7.2(2)
		202.66(5)	1.7(5)		
		207.04(5)	61.5(25)		
4^-	244.1(1)	191.1(2)	0.4(2)	0.0(4)	
3^-	297.88(5)	53.7(2)	0.2(1)	0.2(3)	
		90.90(7)	1.6(2)		
		166.96(5)	9.2(3)		
		244.75(9)	1.5(2)		
		293.51(5)	15.6(7)		
2^-	435.18(5)	137.35(8)	1.1(2)	3.3(7)	6.6(1)
		228.20(5)	16.7(7)		
		382.10(5)	54.8(23)		
		430.81(5)	9.1(5)		
		435.15(5)	4.9(9)		
$1^-,2^-$	569.80(5)	271.92(5)	15.6(7)	3.0(3)	6.6(1)
		362.70(7)	2.5(2)		
		516.70(5)	8.9(4)		
		565.40(7)	3.0(2)		
		569.80(7)	3.1(2)		
$0^-,1^-$	785.55(5)	785.55(5)	4.2(5)	0.2(1)	7.7(2)
$1^-,2$	809.17(5)	374.05(5)	1.2(4)	2.0(3)	6.7(1)
		602.12(5)	1.5(3)		
		804.80(5)	6.2(5)		
		809.15(5)	7.0(5)		
$1^-,2$	935.04(5)	728.07(6)	0.5(1)	0.0(8)	
		930.65(5)	2.0(5)		
		935.02(6)	0.8(1)		
(2^-)	1047.30(5)	477.44(8)	1.2(2)	0.6(3)	7.1(2)
		612.10(8)	1.7(3)		
		749.50(9)	6.9(3)		
		840.20(5)	3.0(3)		
		994.18(5)	19.9(9)		
		1042.91(7)	4.5(3)		
		1047.41(9)	4.2(3)		
$(1^-,2)$	1329.45(5)	759.72(6)	2.8(2)	1.9(2)	6.4(1)
		894.19(6)	3.5(3)		
		1031.30(9)	2.1(3)		
		1122.20(7)	1.9(3)		
		1276.33(5)	9.8(4)		
		1325.00(7)	0.8(2)		

TABLE II. Continuation of Table I.

Level I^π	Level E_{exc} (keV)	γ decay E_γ (keV)	γ decay I_γ (rel.)	Level $P/100$	Level $\log_{10} ft$
2,3	1488.7(1)	1053.3(1)	1.0(2)	0.1(1)	
		1281.7(1)	1.1(2)		
2,3+	1545.80(7)	1248.00(9)	0.4(1)	0.0(2)	
		1492.78(7)	3.9(3)		
2,3+	1622.18(8)	1324.36(7)	1.0(3)	−0.2(2)	
1−,2	2159.90(5)	1590.05(7)	7.2(3)	1.5(1)	6.1(1)
		1952.93(5)	5.3(4)		
1^+	2447.05(5)	287.10(15)	2.7(3)	45(2)	4.4(1)
		824.90(15)	0.7(3)		
		901.22(6)	4.5(3)		
		1117.50(6)	8.3(4)		
		1399.62(5)	37.5(15)	5.7 (Ref.)	
		1511.81(5)	10.0(10)		
		1637.68(5)	7.5(9)		
		1661.35(5)	6.0(6)		
		1877.10(9)	2.7(3)		
		2011.73(5)	59.7(30)		
		2239.92(5)	50.8(22)		
		2393.80(6)	1.1(2)		
		2442.55(5)	100.0(30)		
		2447.1(1)	5.2(5)		
1−,2	2551.1(1)	923.3(2)	0.1(1)	0.7(2)	6.2(1)
		1741.8(1)	2.0(4)		
		2115.9(1)	2.0(3)		
(1^+)	2665.4(1)	1119.8(1)	1.3(3)	8.3(4)	5.0(1)
		1618.6(1)	0.9(3)		
		1730.2(1)	2.0(5)		
		1879.8(1)	1.1(3)		
		2095.6(1)	9.0(4)		
		2661.0(1)	40.1(16)		
1−,2	2796.7(1)	1174.5(2)	0.2(1)	0.9(2)	5.9(1)
		1467.3(2)	0.7(2)		
		2011.2(2)	0.2(1)		
		2226.9(1)	1.2(2)		
		2362.0(2)	0.5(2)		
		2589.7(1)	2.0(3)		
(1^+)	3225.5(1)	2178.1(1)	1.1(3)	0.9(1)	5.5(1)
		2290.2(1)	1.0(3)		
		2439.8(1)	0.8(2)		
		2790.3(1)	3.2(3)		
(1^+)	3365.1(1)	1876.2(2)	1.6(3)	0.9(1)	5.3(1)
		2430.6(3)	0.5(2)		
		2556.7(2)	0.5(2)		
		2579.3(2)	0.6(2)		
		3158.2(1)	1.8(3)		
		3365.1(2)	1.0(3)		

level is supported by two new decays of 759.7 and 894.2 keV, as seen in Fig. 4 in the spectrum gated on the 894.2-keV line. Another spectrum, gated on the 48.7-keV line is displayed in Fig. 5, showing the 516.7-, 1492.8-, and 1590.5-keV decays from the new 569.8-, 1545.8-, and 2159.9-keV levels.

Important new decays, observed in the present work, are seen in Figs. 5 and 6 at 77.8, 167.0, and 271.9 keV. They depopulate the 130.9-, 297.9-, and 569.8-keV levels, respectively. The 569.8-keV level is a new one, introduced in this work but the 130.9-keV level, depopulated by the 77.8-keV line was reported in prompt-γ spectrum following heavy-ion-induced fission [1]. The yrast nature of levels populated in fission [26] is consistent with spin $I = 4$ assignment to the 130.9-keV level proposed in Ref. [1], though one may ask why this level is so well seen, following β decay of the 0^+ ground state of ^{86}Se. It is of interest to check the rate of direct feeding to this level in β decay.

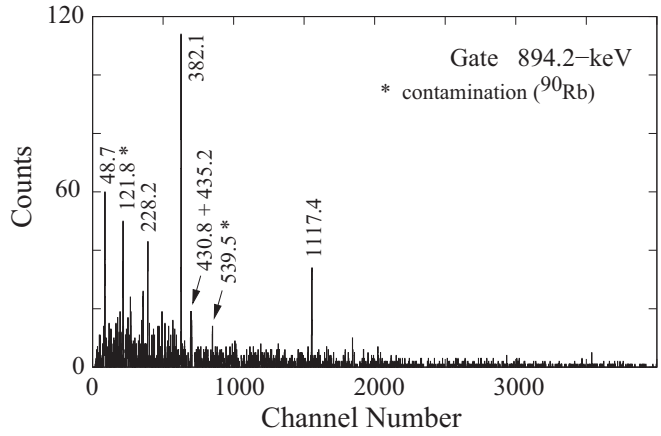

FIG. 4. γ spectrum gated on 894.2-keV line.

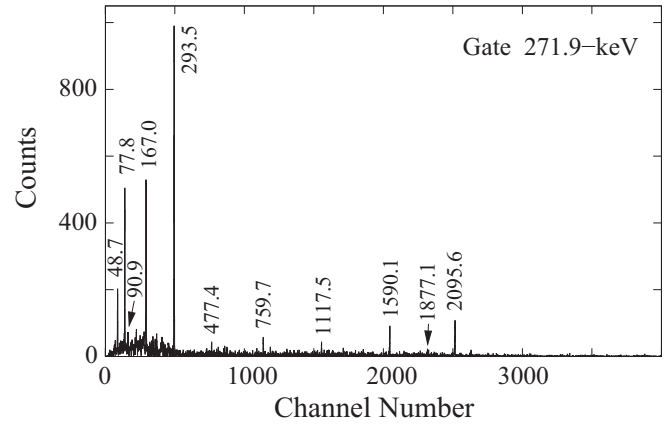

FIG. 6. γ spectrum gated on 271.9-keV line.

1. Population of levels in ^{86}Br in β^- decay of ^{86}Se.

Relative intensities of γ transitions in ^{86}Br observed in β^- decay of ^{86}Se in this work are proportional to intensities reported previously [9,10], except a pronounced difference for the strongest, 2442.5-keV decay, which in our data is nearly factor three less intense. We note that the 2441.1-keV line shown in Fig. 1 of Ref. [10] looks wider than the neighboring lines in that spectrum, while in our data there is a single line at 2442.5 keV. This may be from the different contaminations allowed by the chemical separation technique, applied in Ref. [10], and the electromagnetic separation used in this work.

Using the relative γ intensities shown in Tables I and II we estimated the population of levels in ^{86}Br following β^- decay of ^{86}Se. In the calculation we used the known, total conversion coefficient for the 48.7-keV transition, $\alpha_{tot} = 0.889(21)$ [1,9] as well as new total conversion coefficients, $\alpha_{tot} = 0.29(5)$, 0.18(7), and 0.10(5) for the 77.8-, 153.9-, and 167.0-keV transitions, respectively, determined in this work from the intensity balances observed in the respective, gated γ spectra. The level population values, $P/100$, shown in Tables I and II are normalized to 100 β^- decays, taking as a reference the γ intensity of 5.7 per 100 β^- decays for the 1399.6-keV transition, as reported in Refs. [9,10].

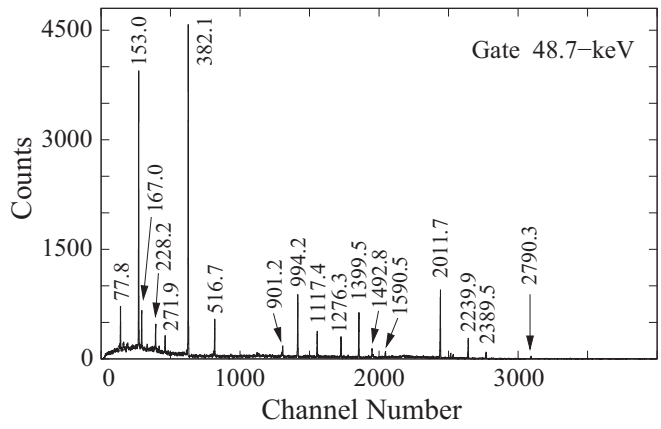

FIG. 5. γ spectrum gated on 48.7-keV line.

The new intensity balances obtained in the present work for the 53.1-, 130.9-, and 297.9-keV levels show negligible (equal to zero within uncertainties) feeding of these levels in β decay of ^{86}Se. The zero feeding of the 130.9-keV level is expected, because of its spin and parity of 4^- [1]. An important, new result is the zero feeding of the 53.1-keV level, which corrects the 12% feeding reported previously [9] and supports the 3^- spin and parity assignment proposed in Ref. [1] for this level. The upper limit for the, unobserved 53.1-keV decay from this level is 0.08 in units of Table I. The strong indirect feeding of the 53.1-keV level could be from the, so-called, structurally controlled γ-ray cascades [27], diverting the decay intensity flow because of similarity of the wave functions of levels in the cascade.

Other important results are the $P/100 = 45(2)$ value for the 1^+ level at 2447.0 keV, and $P/100 = 8.3(4)$ value for the 2665.4-keV level. They are significantly lower than the analogous populations reported before [9,10], which suggest the revision of the ground-state population. We used the procedure proposed in Ref. [28], utilizing the new excitation scheme of ^{86}Br, obtained in this work and the $P/100 = 5.7$ reference value for the 1399.6-keV line, also used in Ref. [28] as the reference to determine the population of the ground state of ^{86}Br in β^- decay of ^{86}Se. For the unknown population of the 4.4-keV level, with the likely spin $I^\pi = 2^-$, we assumed $P/100 = 2(2)$. The new population of the ground state obtained in this work, $P/100(\text{g.s.}) = 39(4)$, is about a factor five larger than reported before [10,28].

2. Spin and parity assignments to levels in ^{86}Br

From the $P/100$ values shown in Tables I and II, we calculated log ft values for levels in ^{86}Br populated in β^- decay of ^{86}Se (using the "Log ft" code provided by the NNDC [29]), which are shown in the last column of Tables I and II. For levels with feeding equal to zero within the uncertainty log ft values were not calculated. The $P/100$ values shown in Table I sum up to 111(7), which is slightly above the 100% limit, possibly because of an uncertainty of the reference value $P/100(1399.6) = 5.7$. We note that rescaling the $P/100$ values from Tables I and II so, that they sum up to 100%, does not change the log ft values shown.

The obtained $\log ft$ values, together with the decay branchings of excited levels served to propose spins and parities, as discussed below. We also used, as the reference, the 3^- spin and parity assignment to the 53.1-keV level and the 4^- assignment to the 130.9- and 244.1-keV levels, discussed above. Furthermore, the $\log ft = 4.4$ for the 2447.0-keV level indicate an allowed character of the corresponding β^- decays and therefore spin and parity 1^+ for this level, as also reported in Refs. [9,10].

The spin and parity of the 4.4-keV level is 2^- because of the low-energy, prompt 48.7-keV decay, which strongly favors a $\Delta I = 1, M1+E2$ multipolarity for this transition. Higher spins are unlikely because of strong decay from the 1^+ level and no decay from the 4^- levels.

Because of low-energy prompt γ decays of the 297.9-keV level to the 4^-, 130.9-, and 244.1-keV levels and to the 2^-, 4.4-keV level, the spin and parity of the 297.9-keV level is 3^-, which is consistent with its zero population in β decay. We also note the lack of any link between the 297.7-keV level and the 1^+, 2447.0-keV level.

The low-energy, 90.9-keV decay of the 3^-, 297.9-keV level to the 207.0-keV level and the strong decay from the 1^+ level, both indicate spin 2 for the 207.0-keV level. The 90.9-keV decay favors a negative parity assignment. The 2^- assignment is consistent with the absence of any decay of this level to the 4^- level at 130.9 keV.

The nonobservation of any decay from the 53.1-keV level to the ground state and the $\log ft = 5.7$ for the ground state implies spin and parity 0^- or 1^- for the ground state. Spin 1^- is favored by the strong decay of the 207.0-keV level to the ground state.

The $\log ft$ values for the 435.2- and 569.8-keV levels are consistent with the 1^- or 2^- assignments to both levels. The 2^- solution for the 435.2-keV level is more likely because of its dominating decay to the 3^- level at 53.1 keV and low-energy decay to the 3^- level at 297.9 keV.

The $\log ft = 5.0$ for the 2665.4-keV level suggests an allowed character of the β^- decay to this level, therefore tentative spin and parity 1^+, as proposed before [9,10]. Decay branches of this level are consistent with this spin assignment.

Tentative spin and parity assignments to other levels, shown in Fig. 3, are based on the feeding and decay branches, observed for these levels in the present work. The proposed spins are consistent with $\log ft$ values for these levels shown in Tables I and II.

B. Excited levels of ^{86}Br populated in ^{235}U fission

The key assignments in ^{86}Br are the 4^- and 7^+ spin and parity for the 130.9- and 1625.5-keV levels, respectively, proposed in Ref. [1]. In the present work we analyzed γ-ray radiation from the cold-neutron-induced fission of ^{235}U, measured with the EXILL array. The intensities of γ lines populated in fission of ^{235}U and their energies are summarized in Table III. Our data agree with that of Ref. [1]. Part of this information is included in Fig. 3 to assist further discussion.

Using the EXILL data we have determined the half-life of the 7^+ level at 1625.5 keV, applying the technique described in detail in our previous work [5]. The procedure gives a half-life of 9.8(5) ns for the 1625.5 level, in accord with the expectation [1]. This value is consistent with an $M2$ multipolarity of the 1049.8-keV transition and an $E3$ multipolarity of the 1494.5-keV transition, with the respective rates of $B(M2;1049.8) = 0.10(2)$ W.u. and $B(E3;1494.5) = 3.4(11)$ W.u.

TABLE III. Levels and their γ decays in ^{86}Br populated in the cold-neutron-induced fission of ^{235}U, as observed in the present work. The energy of the 3^-, 53.12(5)-keV level is adopted from Table I. See text for other comments.

Level I^π	Level E_{exc} (keV)	γ decay E_γ (keV)	γ decay I_γ (rel.)
3^-	53.12(5)	48.70(5)	100(5)
4^-	130.96(15)	77.84(14)	75(5)
4^-	244.08(9)	190.94(6)	80(5)
5^-	575.69(13)	331.61(9)	45(5)
		444.78(15)	12(3)
7^+	1625.48(15)	1049.83(8)	25(5)
		1494.45(15)	6(2)
	2688.7(3)	1063.2(2)	5(2)
	3242.7(3)	1617.2(2)	7(3)

C. Excited levels in ^{86}Kr from β^- decay of ^{86}Br

Low-spin levels of ^{86}Kr were studied before in β^- decay of ^{86}Br [30], reporting the strongly populated level at 4315.8 keV with tentative (2^-) spin assignment [9] and in the $(n,n'\gamma)$ reaction [31]. Medium-spin levels were studied in the (^{7}Li,p2n) reaction [32] and in a fusion-fission reaction [33].

The partial scheme of excited levels in ^{86}Kr, populated in β^- decay of ^{86}Br, as observed in this work, is shown in Fig. 7. Reference [33] has established medium-spin excitations at 3935, 4430, and 4693 keV with spins and parities $5^{(-)}$, $6^{(-)}$, and $7^{(-)}$, respectively, which are included in Fig. 7, to assist further discussion.

In Table IV we show properties of excited levels in ^{86}Kr and their γ decays, as observed in this work. The γ-decay intensities, $I_\gamma/100$, were normalized to 100 β decays, taking the intensity of the 1564.7-keV line $I_\gamma/100 = 62$, as reported in Ref. [9]. The $I_\gamma/100$ values were used to calculate level population per 100 β decays, $P/100$, shown in Table IV.

Figure 8 shows γ spectra gated on lines of ^{86}Kr, populated in β decay of ^{86}Br. In Fig. 8(a) there is a line at 2926.3 keV, corresponding to the direct decay of the 2926.3-keV level to the ground state of ^{86}Kr. Because this decay is important for further discussion we show that the 2926.3-keV line is not from the summation effect of the strong 1361.3- and 1564.7-keV lines present in Fig. 8(a). In Figs. 8(b) and 8(c), we show analogous gated spectra, corresponding to decays of the 3098.9- and 2850.9-keV levels, respectively. In Fig. 8(b) there are strong lines at 1534.3 and 1564.7 keV but there is no line at 3090.0 keV, which would correspond to the summation of the 1534.3- and 1564.7-keV lines. Analogously, these is no summation line at 2851.0 keV in Fig. 8(c). This proves that the summation effect can be neglected.

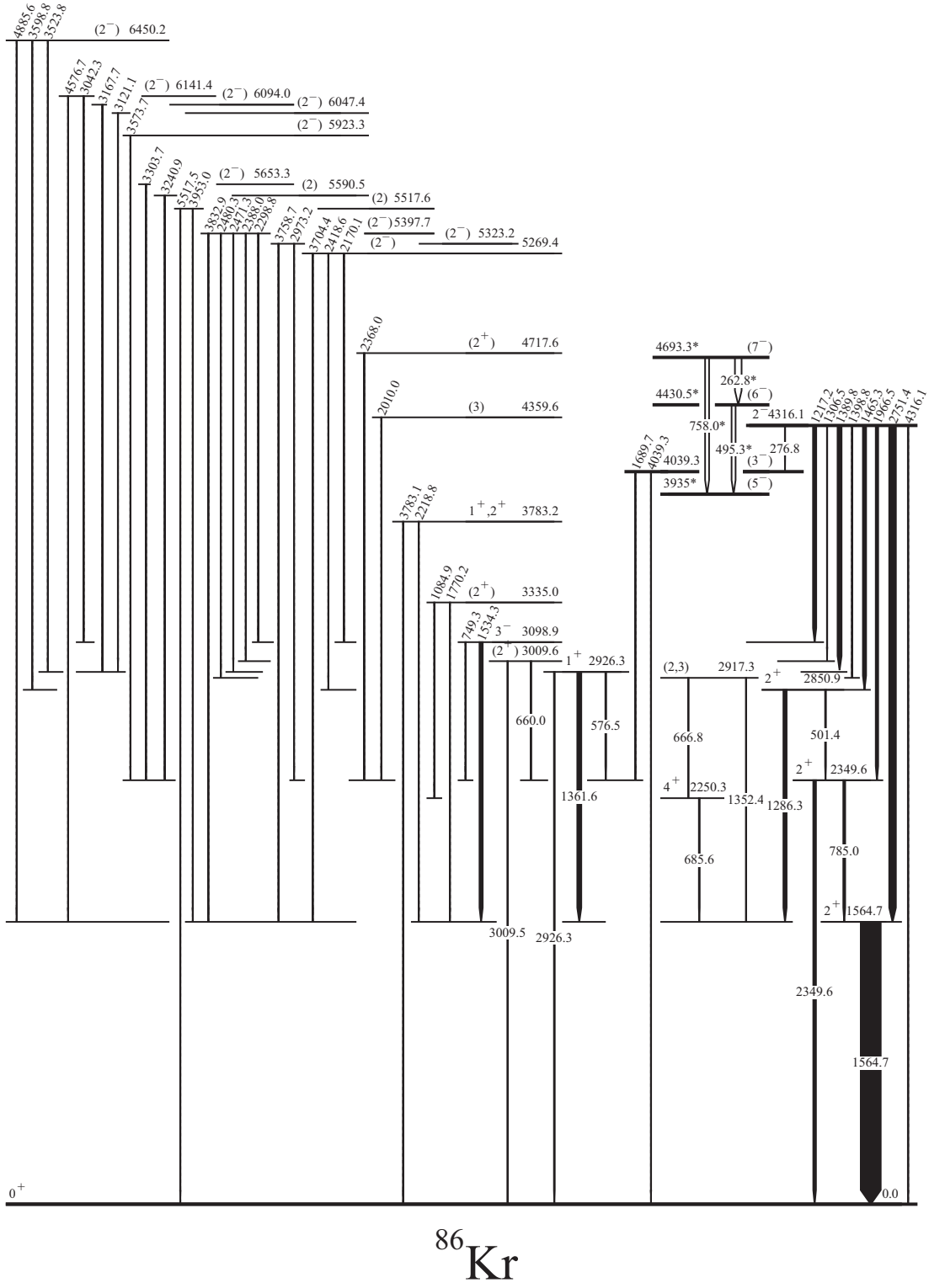

FIG. 7. Level scheme of ^{86}Kr populated in β^- decay of ^{86}Br, as obtained in the present work. Energies of levels and γ decays are given in keV. See Table IV for more information on excited levels and their decays. Levels and transitions marked with a star are drawn after Ref. [9] to assist further discussion.

We introduced new levels at 3335.0, 4359.6, 4717.6, 5653.3, 6047.4, 6094.0, 6141.4, and 6450.2 keV. Some of the transitions, reported in Ref. [9] are moved to other places—the 3758.7 transition depopulates now the 5323.2-keV level, the 2418.6-keV transition depopulates the 5269.4-keV level, and the 2388.0-keV transition depopulates the 5397.7-keV level. The 4316.1-keV decay of the 4316.1-keV level is now firmly established and we add new, 276.8-keV decay of this level.

TABLE IV. Levels and their γ decays in ^{86}Kr, as observed in β^- decay of ^{86}Br in the present work. See text for comments.

Level I^π	Level E_{exc} (keV)	γ decay E_γ (keV)	γ decay $I_\gamma/100$	Level $P/100$	Level $\log_{10} ft$
0^+	0.0			9(5)	7.7(2)
2^+	1564.75(5)	1564.75(5)	62(2)	18(3)	7.0(1)
4^+	2250.27(6)	685.58(5)	1.6(2)	0.0(3)	
2^+	2349.60(5)	784.98(5)	5.0(3)	2.1(9)	7.6(2)
		2349.59(5)	8.4(4)		
2^+	2850.91(5)	1286.25(5)	9.1(4)	0.9(8)	7.8(4)
		501.40(6)	2.1(2)		
(2,3)	2917.27(6)	666.84(6)	0.8(2)	0.3(4)	
		1352.4(2)	0.3(1)		
1^+	2926.27(5)	576.45(8)	0.6(1)	3.2(9)	7.2(1)
		1361.62(5)	11.5(6)		
		2926.28(5)	1.7(2)		
(2^+)	3009.58(7)	659.97(6)	1.1(2)	0.5(4)	8.0(4)
		3009.50(15)	0.6(2)		
3^-	3098.93(5)	749.3(1)	0.2(1)	0.0(8)	
		1534.39(5)	9.0(4)		
(2^+)	3335.0(1)	1084.9(2)	0.4(1)	0.9(3)	7.6(2)
		1770.2(2)	0.5(2)		
$1^+,2^+$	3783.2(2)	2218.8(3)	0.3(1)	0.7(2)	7.5(2)
		3783.1(2)	0.4(1)		
(3^-)	4039.3(1)	1689.7(2)	0.5(2)	0.0(4)	
		4039.3(2)	0.2(1)		
2^-	4316.08(5)	276.8(1)	0.7(2)	58(3)	5.3(1)
		1217.17(5)	9.0(5)		
		1306.5(1)	0.7(2)		
		1389.84(5)	12.1(6)		
		1398.77(5)	0.8(2)		
		1465.25(5)	9.2(5)		
		1966.50(5)	6.2(4)		
		2751.38(5)	18.8(7)		
		4316.1(1)	0.5(2)		
(3)	4359.6(4)	2010.0(4)	0.8(2)	0.1(1)	
(2^+)	4717.6(3)	2368.0(3)	0.3(1)	0.3(1)	7.3(2)
(2^-)	5269.4(1)	2170.1(2)	0.4(2)	1.5(3)	6.3(1)
		2418.6(1)	0.9(1)		
		3704.4(2)	0.2(1)		
(2^-)	5323.2(1)	2973.2(2)	0.5(1)	1.3(2)	6.3(1)
		3758.7(1)	0.6(1)		
(2^-)	5397.7(2)	2298.8(2)	0.1(1)	1.6(4)	6.2(2)
		2388.0(2)	0.5(2)		
		2471.3(2)	0.4(1)		
		2480.3(2)	0.3(1)		
		3832.9(2)	0.3(1)		
(2)	5517.7(2)	3953.0(2)	0.2(1)	0.3(2)	6.8(3)
		5517.6(3)	0.1(1)		
(2)	5590.5(2)	3240.9(2)	0.3(1)	0.3(1)	6.7(2)
(2^-)	5653.3(1)	3303.7(1)	0.6(2)	0.6(2)	6.3(2)
(2^-)	5923.3(2)	3573.7(2)	0.7(2)	0.7(2)	6.0(2)
(2^-)	6047.4(2)	3121.1(2)	0.5(1)	0.3(1)	6.3(2)
(2^-)	6094.0(2)	3167.7(2)	0.3(1)	0.3(1)	6.3(2)
(2^-)	6141.4(2)	3042.3(3)	0.2(1)	0.5(2)	5.9(2)
		3167.7(2)	0.3(1)		
(2^-)	6450.2(1)	3523.8(2)	0.2(1)	0.7(2)	5.4(2)
		3598.8(2)	0.3(1)		
		4885.6(1)	0.2(1)		

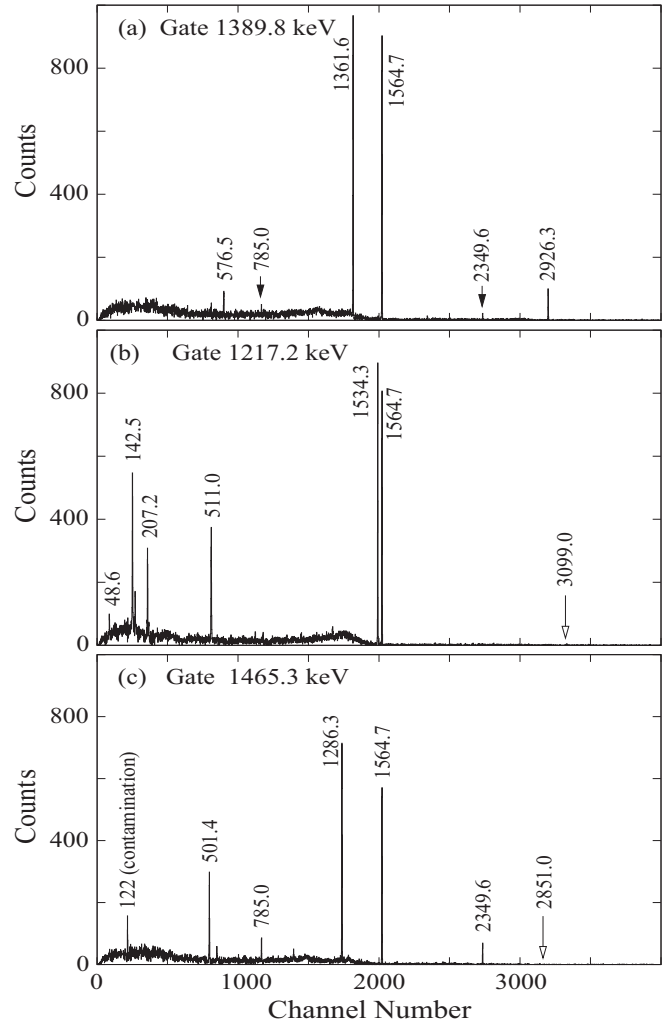

FIG. 8. γ spectrum gated on the (a) 1389.8-keV line, (b) 1217.2-keV line, and (c) 1465.3-keV line.

Of the previously reported but unplaced transitions [9], the 749.3-, 2471.3-, 2973.2-, 3240.9-, 3573.7- and 4885.6-keV transitions are assigned to ^{86}Kr while the 803.3-, 899.8-, and 3064.4-keV transitions are not confirmed. We could not confirm the 6089.1-, 6160.5-, 6211.8-, 6720.5-, and 6768.3-keV levels reported previously [9,30].

1. Population of levels in ^{86}Kr in β^- decay of ^{86}Br.

Relative intensities of γ transitions in ^{86}Kr observed in β^- decay of ^{86}Br in this work are similar to those reported before [9], with small but important differences.

The new intensity balance obtained in the present work for the 4^+, 2250.3-keV level shows zero feeding of this level in β decay of ^{86}Br. This is consistent with the 0^- or 1^- spin and parity of the ground state in ^{86}Br proposed in Sec. II A 2 as well as the lack of any $I > 1$, beta decaying isomer in ^{86}Br. We also note the low feeding in β decay of the 3098.9-, 4039.3-, and 4359.6-keV levels, which may indicate spin $I > 2$ for these levels.

The sum of all $P/100$ values for excited levels, shown in Table IV yields 91(5). Therefore, we propose that the feeding

of the ground state of ^{86}Kr in β decay of the ground state of ^{86}Br is $P/100 = 9(5)$.

The populations, $P/100$, for levels in ^{86}Kr, shown in Table IV were used to calculate log ft values, which are displayed in the last column of Table IV. For levels with feeding equal to zero within uncertainty log ft values were not calculated. The present log ft values agree with the literature values [9] within uncertainties.

Finally, it is interesting to note that the time spectrum of the type shown in Fig. 2, gated on the 685.6-keV line depopulating the known 4^+ level in ^{86}Kr is similar to the time spectrum gated on the 1564.7-keV, shown in Fig. 2(c) and does not indicate any presence in ^{86}Br of a hypothetical, β decaying, 5-s isomer with spin $I > 1$.

2. *Spin and parity assignments to levels in* ^{86}Kr

The high cumulative yield for ^{86}Br in fission of ^{235}U +n allowed precise measurements of angular correlations in $\gamma\gamma$ cascades of ^{86}Kr, populated in β decay of ^{86}Br. The eight EXOGAM Clover detectors of EXILL, mounted in one plane in an octagonal geometry, provided three angles θ of 0°, 45°, and 90° for angular correlation analysis. Further comments on the technique can be found in Refs. [5,23,39]. In the following analysis of angular correlations we used formulas and conventions of Refs. [36,37].

Experimental angular correlations can be expanded into a series of Legendre polynomials $P_k(\cos\theta)$,

$$W(\theta) = \sum_k a_k P_k(\cos\theta). \quad (1)$$

Because $P_0(\cos(90^\circ)) = 1$, it is convenient to normalize the formula (1) so that $W(90^\circ) = 1$. For the case limited to dipole and quadrupole transitions the normalized formula reads

$$W(\theta) = 1 + (a_2/a_0)P_2(\cos\theta) + (a_4/a_0)P_4(\cos\theta). \quad (2)$$

Analogous theoretical angular correlations are expressed as [36,37]

$$W(\theta) = 1 + A_2B_2P_2(\cos\theta) + A_4B_4P_4(\cos\theta). \quad (3)$$

Therefore, the experimentally derived a_k/a_0 coefficients can be compared to theoretical A_kB_k coefficients, defined in Refs. [36,37], which depend on spins of levels and multipolarities of transitions in the cascade and, in particular, on the mixing ratios, δ_1 and δ_2 of the upper and lower transition in the cascade, respectively.

Figure 9 shows the angular-correlation analysis for the 2751.4- to 1564.7-keV cascade in ^{86}Kr, assuming the spin of the 4316.1-keV level to be (a) $I = 1$, (b) $I = 2$ or (c) $I = 3$. The ellipses in the upper panels of Figs. 9(a)–9(c) represent theoretical values of A_2B_2 and A_4B_4 coefficients for the assumed spin hypothesis as a function of the mixing ratio δ_1 of the 2751.1-keV transition, which varies from 0 to $\pm\infty$ (red dots) along the two branches of the "ellipse" (the 1564.7-keV transition is an unmixed, stretched quadrupole with $\delta_2 = 0$). The experimental values of a_2/a_0 and a_4/a_0 with their error bars are represented by rectangle boxes (blue). Lower panels show plots of the χ^2 function per degree of freedom. There are two solutions for the 2751.4- to 1564.7-keV cascade, seen in

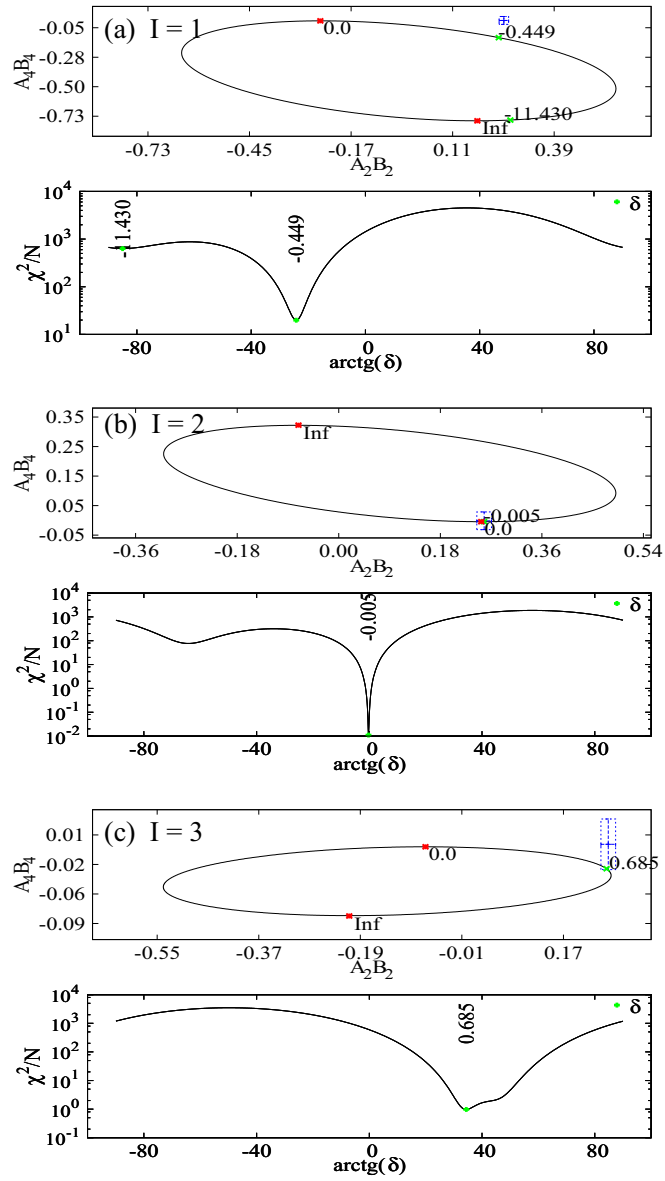

FIG. 9. Angular correlations analysis for the 2751.4- to 1564.7-keV cascade in ^{86}Kr, for the (a) $I = 1$, (b) $I = 2$, and (c) $I = 3$ spin assignment to the 4316.1-keV level.

Figs. 9(b) and 9(c) for spins $I = 2$ and $I = 3$, with mixing ratios of the 2751.4-keV transition, $\delta = -0.1(2)$ and $\delta = 0.69(9)$, respectively. The $I = 1$ spin hypothesis is rejected by the χ^2 analysis, as shown in Fig. 9(a).

Figure 10 shows another important angular correlation. The analysis for the 1361.6- to 1564.7-keV cascade indicates that the allowed spins for the 2926.3-keV level are $I = 1$ and $I = 3$, while the $I = 2$ solution reported previously [9] is clearly rejected by the correlations.

Results of the analysis for $\gamma\gamma$ cascades in ^{86}Kr are presented in Table V, showing experimental a_k/a_0 coefficients and δ mixing ratios derived for various spin hypotheses.

In several cases it was also possible to determine linear polarization of γ transitions by measuring directional-linear-polarization correlations in $\gamma\gamma$ cascades, using the EXOGAM

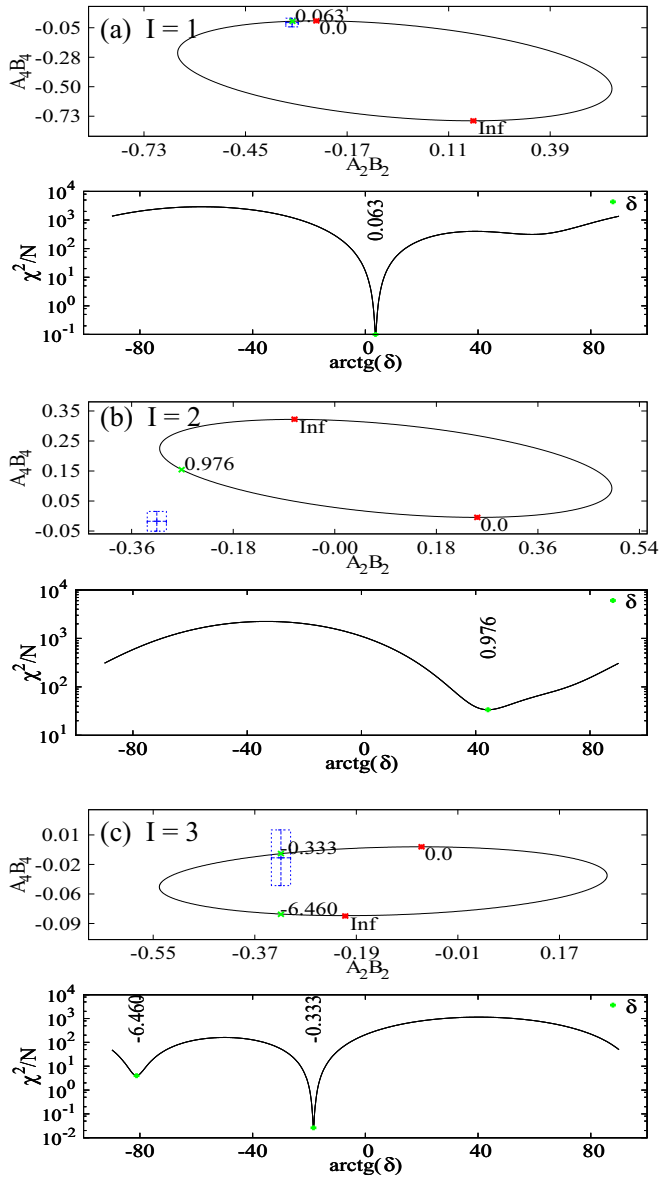

FIG. 10. Angular correlation analysis for the 1361.6- to 1564.7-keV cascade in ^{86}Kr for the (a) $I = 1$, (b) $I = 2$, and (c) $I = 3$ spin assignment to the 2926.3-keV level.

Clover detectors as Compton polarimeters. For the polarization sensitivity calibration of the EXOGAM Clovers we took the results of Ref. [34] reporting the polarization sensitivity for the Eurogam Clover detectors [35]. The 1564.7-keV stretched quadrupole decay of the first 2^+ level in ^{86}Kr [9] served as a known, reference transition in a $\gamma\gamma$ cascade. Results of the linear polarization analysis for several γ transitions in ^{86}Kr are shown in Table VI in the column $P_{\rm exp}(\gamma^p)$.

The last column of Table VI shows theoretical values of linear polarization $P_{\rm th}(\gamma^p)$, which for a mixed dipole-plus-quadrupole transition can be calculated for the upper transition in a cascade from the formula,

$$P_{\rm th}(\gamma_1) = \pm \frac{3A_2B_2 + \frac{5}{4}A_4B_4 + 4A_2(\gamma_2)\frac{2\delta_1 F_2(12I_0I_1)}{1+\delta_1^2}}{2 - A_2B_2 + \frac{3}{4}A_4B_4}. \quad (4)$$

TABLE V. Normalized, experimental angular-correlation coefficients, a_k/a_0, and the corresponding mixing ratios δ of γ transitions in ^{86}Kr, populated in β^- decay of ^{86}Br, determined for various spin hypotheses. The 1564.7-keV transition is a stretched quadrupole with $\delta(\gamma_2) = 0.0$.

Cascade $\gamma_1 - \gamma_2$	a_2/a_0 (expt.)	a_4/a_0 (expt.)	Spins I_1, I_2, I_3	$\delta(\gamma_1)$
501.4–2349.6	0.23(11)	0.13(27)		
$\delta(\gamma_2)$=0.00			$2 \to 2 \to 0$	0.03(20)
				$-2.3(^{+0.8}_{-1.5})$
			$3 \to 2 \to 0$	$0.5(^{+1.5}_{-0.3})$
				$1.1(^{+1.0}_{-0.2})$
685.6–1564.7	0.098(5)	−0.08(11)	$4 \to 2 \to 0$	0.0
785.0–1564.7	0.318(45)	0.04(10)	$2 \to 2 \to 0$	−0.10(7)
			$3 \to 2 \to 0$	0.82(23)
1217.2–1534.3	0.362(23)	0.051(56)		
$\delta(\gamma_2)$=0.01			$2 \to 1 \to 2$	No solution
$\delta(\gamma_2)$=0.01			$2 \to 3 \to 2$	0.75(30)
1286.3–1564.7	−0.092(3)	0.016(54)	$2 \to 2 \to 0$	0.47(5)
			$3 \to 2 \to 0$	−0.03(3)
1352.4–1564.7	−0.31(13)	−0.54(25)	$2 \to 2 \to 0$	2.8(18)
1361.6–1564.7	−0.319(17)	−0.013(33)	$1 \to 2 \to 0$	0.06(2)
			$2 \to 2 \to 0$	No solution
			$3 \to 2 \to 0$	−0.33(3)
1389.8–1361.6	−0.01(2)	−0.03(4)		
$\delta(\gamma_2)$=0.06			$2 \to 1 \to 2$	0.12(20)
				2.3(10)
$\delta(\gamma_2)$= −0.33			$2 \to 3 \to 2$	−0.18(3)
1389.8–2926.3	−0.004(65)	0.01(14)		
$\delta(\gamma_1)$= 0.12	or 2.3		$2 \to 1 \to 0$	any $\delta(\gamma_2)$
1465.3–1286.3	0.363(31)	−0.039(75)		
$\delta(\gamma_2)$=0.47			$2 \to 2 \to 2$	−0.03(4)
				−2.1(2)
$\delta(\gamma_2)$=−0.03			$2 \to 3 \to 2$	0.36(8)
				1.5(2)
1534.3–1564.7	−0.066(19)	0.042(41)	$2 \to 2 \to 0$	0.43(3)
			$3 \to 2 \to 0$	0.01(2)
1966.5–2349.6	0.224(31)	−0.021(75)		
$\delta(\gamma_2)$=0.00			$2 \to 2 \to 0$	0.04(4)
			$3 \to 2 \to 0$	0.53(15)
				1.3(3)
2751.4–1564.7	0.254(13)	0.003(30)	$1 \to 2 \to 0$	No solution
			$2 \to 2 \to 0$	0.01(2)
			$3 \to 2 \to 0$	0.61(8)
3758.7–1564.7	0.38(14)	0.12(33)	$2 \to 2 \to 0$	−0.2(3)
			$3 \to 2 \to 0$	0.82(45)
4885.6–1564.7	0.34(8)	−0.00(18)	$2 \to 2 \to 0$	−0.12(13)
			$3 \to 2 \to 0$	0.84(35)

In formula (4) the "+"("−") sign applies to the $M1{+}E2$ ($E1{+}M2$) multipolarity of the studied γ transition. Therefore, comparing the sign of the calculated and the experimental polarization, one can distinguish between the $M1{+}E2$ and $E1{+}M2$ multipolarity of this transition. The A_k, B_k, and F_2, coefficients are given in Ref. [36].

Formula (4), which to our knowledge was not reported before, describes the case when the lower transition in a cascade is known and the upper one studied, as illustrated

TABLE VI. Experimental $P_{exp}(\gamma^p)$ and calculated $P_{th}(\gamma^p)$ values of linear polarization for γ^p transitions in ^{86}Kr, populated in β^- decay of ^{86}Br, as obtained in the present work. See text for further explanation.

Cascade $\gamma_1 \rightarrow \gamma_2$	$P_{exp}(\gamma^p)$	Spins in cascade	Parity of γ^p	$P_{th}(\gamma^p)$
685.6^p–1564.7	0.25(15)	$4 \rightarrow 2 \rightarrow 0$	$E2$	0.10(5)
785.0^p–1564.7	0.6(3)	$2 \rightarrow 2 \rightarrow 0$	$M1+E2$	0.44(12)
1286.3^p–1564.7	0.4(2)	$2 \rightarrow 2 \rightarrow 0$	$M1+E2$	0.42(5)
		$3 \rightarrow 2 \rightarrow 0$	$E1+M2$	0.19(15)
1286.3 - 1564.7^p	−0.48(22)	$I_0 \rightarrow 2 \rightarrow 0$	$E2$	−0.12(3)
1361.6^p–1564.7	−0.58(15)	$1 \rightarrow 2 \rightarrow 0$	$M1+E2$	−0.48(5)
		$3 \rightarrow 2 \rightarrow 0$	$M1+E2$	−0.99(8)
1361.6–1564.7^p	−0.28(12)	$I_0 \rightarrow 2 \rightarrow 0$	$E2$	−0.42(3)
1534.3^p–1564.7	0.15(10)	$2 \rightarrow 2 \rightarrow 0$	$M1+E2$	0.21(8)
		$3 \rightarrow 2 \rightarrow 0$	$E1+M2$	0.06(4)
1534.3–1564.7^p	−0.13(10)	$I_0 \rightarrow 2 \rightarrow 0$	$E2$	−0.07(3)
1966.5^p–2349.6	−0.5(3)	$2 \rightarrow 2 \rightarrow 0$	$E1+M2$	−0.42(8)
1966.5 - 2349.6^p	0.3(2)	$I_0 \rightarrow 2 \rightarrow 0$	$E2$	0.36(6)
2751.4^p–1564.7	−0.42(8)	$2 \rightarrow 2 \rightarrow 0$	E1+M2	−0.45(5)
2751.4–1564.7^p	0.33(8)	$I_0 \rightarrow 2 \rightarrow 0$	E2	0.44(3)

in Fig. 11(a). This most commonly encountered situation is not intuitive because the polarization is measured for the γ_1 transition depopulationg an *unoriented* state. The "obvious" case described in the literature [37,38] is the one shown in Fig. 11(b), where first one observes a γ_1 transition (GATE ON γ_1), which aligns spins of the intermediate state with spin I_1. This alignment, described by coefficients $B_k(\gamma_1,\delta_1)$, induces an anisotropy and a polarization of the γ_2 transition. The anisotropy is described by coefficients $A_k(\gamma_2,\delta_2)$. For the polarization-sensitive measurement an additional dependence on δ_2 and $B_2(\gamma_1)$ appears and the linear polarization of the lower transiting in a cascade can be calculated from the formula [37],

$$P_{th}(\gamma_2) = \pm \frac{3A_2B_2 + \frac{5}{4}A_4B_4 - 4B_2(\gamma_1)\frac{2\delta_2 F_2(12I_2I_1)}{1+\delta_2^2}}{2 - A_2B_2 + \frac{3}{4}A_4B_4}, \quad (5)$$

where again the "+"("−") sign applies to the $M1+E2$ ($E1+M2$) multipolarity of the studied γ transition.

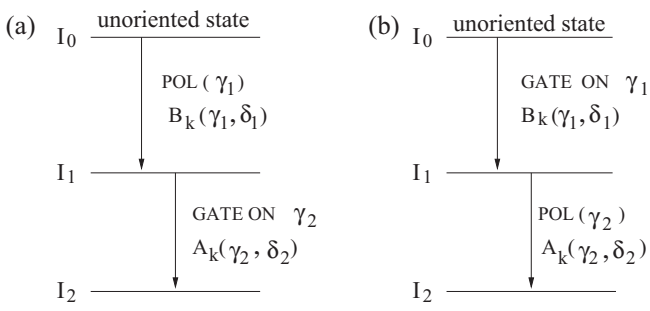

FIG. 11. Schematic directional-polarization correlations for the case of gating (GATE) on the (a) lower or (b) upper transition in the cascade. Polarization (POL) is then measured for the (a) upper or (b) lower transition.

Formula (4) was derived in a similar way as formula (5), using general equations and guidelines provided in Ref. [37]. For mixed transitions the additional dependence of linear polarization on the δ ratio in formulas (4) and (5) allows the rejection of some of the δ solutions provided by angular correlations. In case the polarization is calculated for an unmixed transition ($\delta = 0$) both formulas are identical, though formula (4) gives polarization of γ_1 while formula (5) gives polarization of γ_2.

The polarization for transitions in a cascade where angular correlations have been measured can be calculated using the experimental δ and taking the experimental a_k/a_0 coefficients instead of A_kB_k. The values shown in the last column of Table VI were calculated for the polarity shown in column 4 of Table VI using a_k/a_0 and δ values for γ_1 from Table V.

Spin and parity assignments to levels in ^{86}Kr, shown in Fig. 7 have been proposed taking into account angular correlations, linear polarization, decay branchings, and $\log ft$ values obtained in the present work.

For the 2751.4-keV transition spins $I = 2$ and $I = 3$ with both $M1+E2$ and $E1+M2$ multipolarities are allowed by angular correlations. To determine the parity of the 4316.1-keV level we have derived the linear polarization of the 2751.4-keV transition from the directional-polarization correlations in the 2751.4- to 1564.7-keV cascade. The resulting experimental polarization, $P_{exp} = -0.42(8)$ agrees with the $P_{th} = -0.45(3)$ value shown in Table VI for spin $I = 2$ hypothesis, assuming an $E1+M2$ multipolarity. Spin and parity solutions 2^+, 3^+, and 3^- are rejected by the experimental polarization. This uniquely indicates the $I^\pi = 2^-$ spin and parity for the 4316.1-keV level. We note that the experimental (gated on the 2751.4-keV line) and the calculated [from formula (5)] linear polarizations of the 1564.3-keV, stretched $E2$ transition also agree when taking spin $I^\pi = 2^-$ for the 4316.1-keV level.

With $I^\pi = 2^-$ spin and parity of the 4316.1-keV level, obtained above, one can exclude the 0^- spin and parity hypothesis for the ground state of ^{86}Br, considering the $\log ft = 5.3$ of the 4316.1-keV level. Thus, spin and parity of the ground state of ^{86}Br is 1^-.

For the 2250.3-keV level angular correlations provide one solution with spin $I = 4$. Positive parity results from the prompt character of the 685.6-keV transition. The linear polarization is consistent with this solution.

For the 2349.6-keV level the measured polarization of the 785.0-keV transition value fits the polarization calculated for the $I^\pi = 2^+$ spin and parity, only. Furthermore, the experimental (gated on the 2349.6-keV line) and calculated [from formula (4)] linear polarization of the 1966.5-keV transitions agree with assignments of $I^\pi = 2^+$ for the 2349.6-keV level and $I^\pi = 2^-$ for the 4316.1-keV level. The experimental (gated on the 1966.5-keV line) and calculated [from formula (5)] linear polarization of the 2349.6-keV transition also agree, within uncertainty, when taking spin and parity $I^\pi = 2^+$ for the 2349.6-keV level and this is the only solution.

For the 2850.9-keV level spin (2,3) and firm, positive parity are reported [9]. Our angular correlations and linear polarization allow spin and parity of 2^+ or 3^-. Therefore we assign spin and parity 2^+ to this level.

For the 2917.3-keV level spin and parity of (3^-) is reported in Ref. [9]. The observed branchings are consistent with spin 3, though, angular correlations for the suggest spin $I = 2$ for this level.

The angular correlations and linear polarization for the 1361.6- to 1564.7-keV cascade, provide the unique $I^\pi = 1^+$ solution for the 2926.3-keV level. This is an important new result, which will be discussed further in the text.

A spin and parity 3^- of the 3098.9-keV level, firmly assigned in Ref. [9], is supported by the present data. The very anisotropic angular correlation in the 1217.3- to 1534.3-keV cascade allow the rejection of the spin $I = 1$ hypothesis for the 3098.9-keV level.

Tentative spin and parity assignments to other levels, shown in Fig. 7, were proposed based on their decay branchings and $\log ft$ values. In particular we note the spin and parity (3^-) assignment to the 4039.3-keV level, proposed considering its zero β feeding and the low-energy link to the 2^-, 4316.2-keV level. This result tightens up the previous assignment of $(2,3)^-$ [9]. Also the (2^-) assignment for the 6450.2-keV level, consistent with the $\log ft = 5.4$ of this level is worth noting.

III. DISCUSSION

A. General remarks

Any interpretation of the β-decay schemes of ^{86}Se and ^{86}Br has to account for high populations of the 1^+, 2447.0-keV level in ^{86}Br and the 2^-, 4316.1-keV level in ^{86}Kr. Strong $E1$ decays from 1^+ levels in odd-odd nuclei of the region also need proper explanation [15].

Orbitals near the Fermi level in ^{86}Br are the $p_{3/2}$ and $f_{5/2}$ protons and the $d_{5/2}$ neutrons. At low excitation energies one expects two overlapping multiplets, $(\pi p_{3/2}, \nu d_{5/2})_j$ and $(\pi f_{5/2}^{-1}, \nu d_{5/2})_j$ with spin j ranging from 1^- to 4^- and from 0^- to 5^-, respectively.

Medium-spin, yrast excitations in ^{86}Br are formed by the odd proton promoted to the $g_{9/2}$ orbital, producing the $(\pi g_{9/2}, \nu d_{5/2})_j$ multiplet with spin j from 2^+ to 7^+. When, in addition, the odd neutron is promoted to the $g_{7/2}$ orbital the $(\pi g_{9/2}, \nu g_{7/2})_j$ multiplet is formed with the 1^+ and 8^+ members at the bottom of the multiplet. Yrast, 8^+ levels are observed in the discussed region in odd-odd nuclei ^{88,92,94}Rb [1,40,41], and 1^+ levels, strongly populated in β decay, are reported in ^{88}Br [10], in ^{88,90,92,94}Rb [15,17], and in ^{92,94}Y [13,16].

Low-spin levels in ^{86}Kr are from excitations of the $p_{3/2}$ or $f_{5/2}$ protons. When a proton is further promoted to the $g_{9/2}$ orbital the negative-parity $\pi(p_{3/2}, g_{9/2})_j$ and $\pi(f_{5/2}, g_{9/2})_j$ multiplets are formed with spin j, ranging from 3^- to 6^- and from 2^- to 7^-, respectively.

At medium energies in both nuclei one may also expect excitations involving the $p_{1/2}$ proton (and the $s_{1/2}$ neutron in ^{86}Br). As argued in the recent study of ^{86}Ge $\rightarrow$ ^{86}As $\rightarrow$ ^{86}Se β decays [18], there should also be excitations populated in the Gamow-Teller decay of the core $p_{1/2}$ neutrons to the $p_{3/2}$ protons.

The $\log ft = 4.4$ of the 2447.0-keV level in ^{86}Br is consistent with the allowed decay, only. The $\nu g_{7/2} \rightarrow \pi g_{9/2}$ Gamow-Teller decay is clearly observed at $N > 56$, where the $g_{7/2}$ neutron is well populated, resulting in the $\log ft \approx 4.0$ for the 1^+, 988.4-keV level in ^{94}Rb [17]. In lighter Rb isotopes the population of $g_{7/2}$ neutrons decreases, resulting in $\log ft \approx 4.5$, as illustrated in Fig. 4 of Ref. [17] and Fig. 5 of Ref. [15].

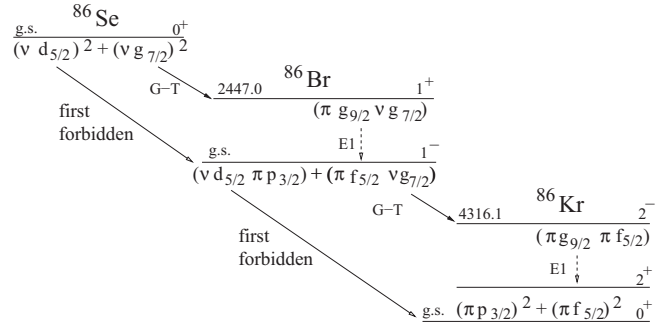

FIG. 12. Schematic drawing of the proposed decay scenario in $A = 86$ isobars, involving the $\nu g_{7/2} \rightarrow \pi g_{9/2}$, G-T decay.

For β decays of ^{86}Se and ^{86}Br we propose a scenario sketched in Fig. 12. Here, the G-T decay of the $g_{7/2}$ neutron admixed in the ground state of ^{86}Se and ^{86}Br, populates preferably the $(\pi g_{9/2}, \nu g_{7/2})_{1^+}$ and $(\pi g_{9/2}, \pi f_{5/2})_{2^-}$ configurations in ^{86}Br and ^{86}Kr, respectively. As shown in Fig. 7, with the (3^-), 4039.3-keV level proposed in this work, there is now a nearly complete multiplet of levels, corresponding to the $\pi(f_{5/2}^{-1}, g_{9/2})_j$ configuration, supporting the proposed interpretation of the 4316.2-keV, 2^- level as a member of this multiplet. At the same time, the first forbidden decay of the $d_{5/2}$ neutron, the major neutron component in the ground states of ^{86}Se and ^{86}Br, to the $f_{5/2}$ or $p_{3/2}$ proton, explains β decays to ground states and low-energy states.

In the past other scenarios for β decays in the $A = 86$ and $A = 88$ mass chains were considered, allowing the G-T decay of the core $p_{1/2}$ neutron to the $p_{3/2}$ valence proton, only [14,15]. We note that the authors of Refs. [14,15] were unsatisfied with their propositions. The $\nu g_{7/2} \rightarrow \pi g_{9/2}$ G-T decay seems to be a better option, also because it allows one to explain the pronounced $E1$ transitions from the 2447.0-keV, 1^+ and 4316.2-keV, 2^- levels as because of the $\pi g_{9/2} \rightarrow \pi p_{3/2}$ or $\nu g_{7/2} \rightarrow \nu s_{1/2}$ transitions, enhanced by the octupole coupling between the $g_{9/2}$ and the $f_{5/2}$ or $p_{3/2}$ protons. This is more natural than the scenario proposed previously [15], involving the $f_{5/2}^{-1}$, neutron hole from the core or the $d_{5/2}$ proton particle from the $Z > 50$ shell in the $\nu d_{5/2} \rightarrow \nu f_{5/2}^{-1}$ or $\pi d_{5/2} \rightarrow \pi f_{5/2}^{-1}$ $E1$ decays, respectively.

One may argue that the $\nu g_{7/2} \rightarrow \pi g_{9/2}$ G-T decay is likely at $N > 56$, where the $g_{9/2}$ proton is close to the Fermi level whereas near $N = 50$ the $\nu p_{1/2} \rightarrow \pi p_{3/2}$ decay should prevail. However, the systematics of excitation energies of 1^+ levels populated in G-T decays in the region shown in Fig. 13 suggests that all the 1^+ levels have some common ground. In Fig. 13(a) the 1^+ excitation energy in the $N = 51$ and $N = 53$ isotones grows monotonically when moving towards lower Z. This can be explained as from the departure of the $g_{9/2}$ proton orbital from the Fermi level, when assuming the

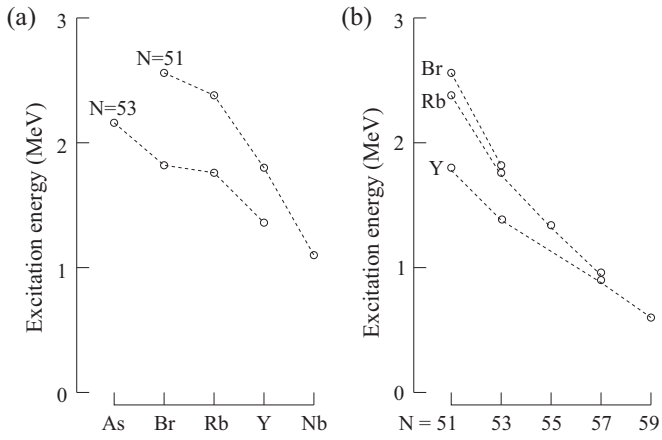

FIG. 13. Energies of strongly populated 1^+ levels in odd-odd (a) $N = 51$ and $N = 53$ isotones and (b) Br, Rb, and Y isotopes.

$(\nu g_{7/2},\pi g_{9/2})_{1^+}$ contribution in the wave functions of these 1^+ levels. Analogously, in Fig. 13(b) the 1^+ excitation energy grows monotonically in Br, Rb, and Y isotopes, when moving towards lower N, but now because of the departure of the $g_{7/2}$ neutron orbital from the Fermi level. Both trends are consistent with the $(\nu g_{7/2},\pi g_{9/2})_{1^+}$ coupling present in wave functions of the discussed 1^+ levels down to $N = 51$ and $Z = 35$. We note that the $(\nu p^{-1}_{1/2},\pi p_{3/2})_{1^+}$ coupling, proposed in Refs. [13–15,18] is clearly inconsistent with Fig. 13(b) and also, partly with Fig. 13(a), where it could not explain the energy drop from Y to Nb.

B. Shell-model calculations

To verify quantitatively the scenario proposed in Fig. 12, we have conducted large-scale, shell-model calculations of excitations in ^{86}Br and ^{86}Kr using the coupled-scheme code NATHAN [43]. The calculations have been performed in a valence space including the $(1f_{5/2},2p_{3/2},2p_{1/2},1g_{9/2})$ orbitals for protons and the $(2d_{5/2},3s_{1/2},1g_{7/2},2d_{3/2},1h_{11/2})$ orbitals for neutrons, outside the ^{78}Ni inert core. The effective interaction was described in Refs. [2,42] and used recently in Refs. [4–6]. In our previous study of the odd-odd ^{86,88}Br [5] a fair agreement was found between the shell model and the experiment, though the ordering of the members of the $(\pi p_{3/2}\nu d_{5/2})$ and $(\pi f^{-1}_{5/2}\nu d_{5/2})$ multiplets was not consistent with experimental assignments. The ground state of ^{88}Br predicted by the shell model was 3^- and the 1^- level was located 60 keV above, while in the experiment the 3^- level is placed 273 keV above the 1^- level. Furthermore, in ^{86}Br the shell model predicted 4^- level as the ground state with the 1^- state 300 keV higher (see Figs. 12 and 13 of Ref. [5]). Because there is now a convincing evidence for the 1^- ground state in, we have fine-tuned the proton-neutron $V_{d5/2,p3/2}$ and $V_{d5/2,f5/2}$ matrix elements to obtain a more accurate reproduction of these multiplets in both odd-odd bromine isotopes. The corrections allowed one to invert of the order of the calculated states in ^{86}Br and ^{88}Br, while preserving the physics of $N = 50$ nuclei (proton-proton interaction was not modified) and of the even-even and even-odd nuclei studied previously [2–4,7,8].

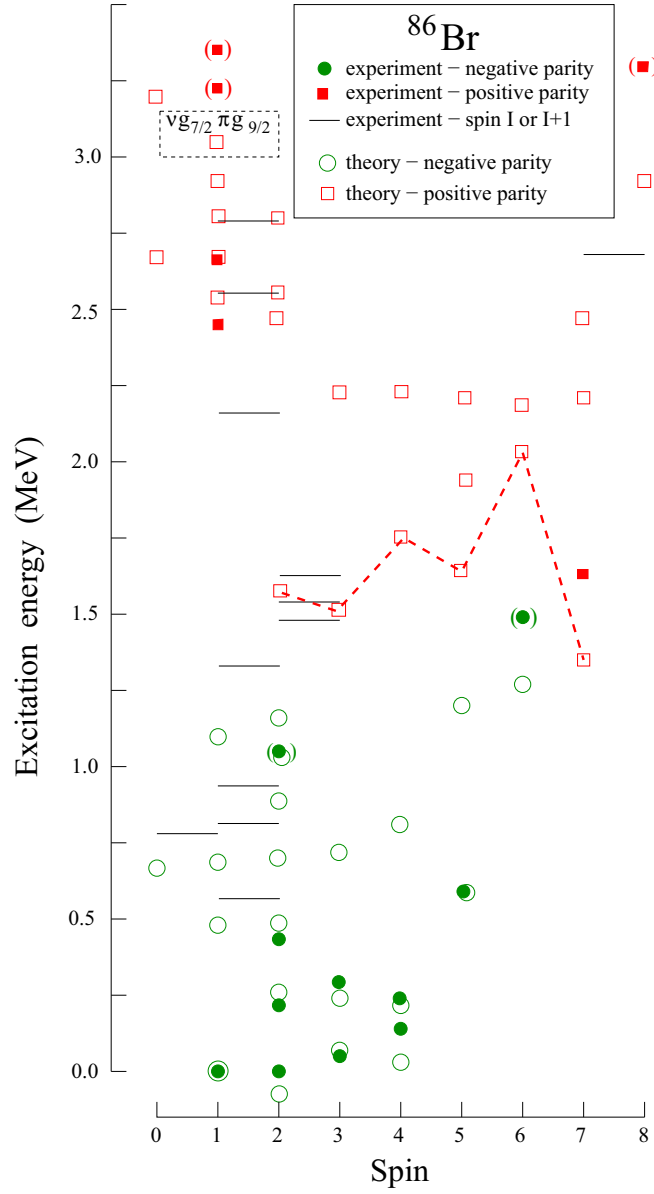

FIG. 14. Comparison of calculated and experimental levels in ^{86}Br. Calculations are normalized to the experiment at the ground-state level. See text for more comments.

The results of the present calculations for ^{86}Br and ^{86}Kr are shown in Figs. 14 and 15, respectively. The scale of the observed excitations of 3.5 MeV in ^{86}Br and 6.5 MeV in ^{86}Kr is reproduced correctly. Similarly as observed in the calculations for the $A = 88$, 90 mass chains [5,6], low-energy levels in ^{86}Br have negative parity and are from $(\pi p_{3/2},\nu d_{5/2})_{1^-,\ldots,4^-}$ and $(\pi f^{-1}_{5/2},\nu d_{5/2})_{0^-,\ldots,5^-}$ excitations, while the positive-parity levels appear only above 1.3 MeV, when the proton is elevated to the $g_{9/2}$ orbit. In contrast, in ^{86}Kr, negative-parity levels appear when the proton pair is broken. The first 3^- level, dominated by the $\pi(p_{3/2},g_{9/2})$ component, is located at 2.6 MeV and the first 4^- state, based on the $\pi(f^{-1}_{5/2},g_{9/2})$ configuration, lies 1 MeV higher.

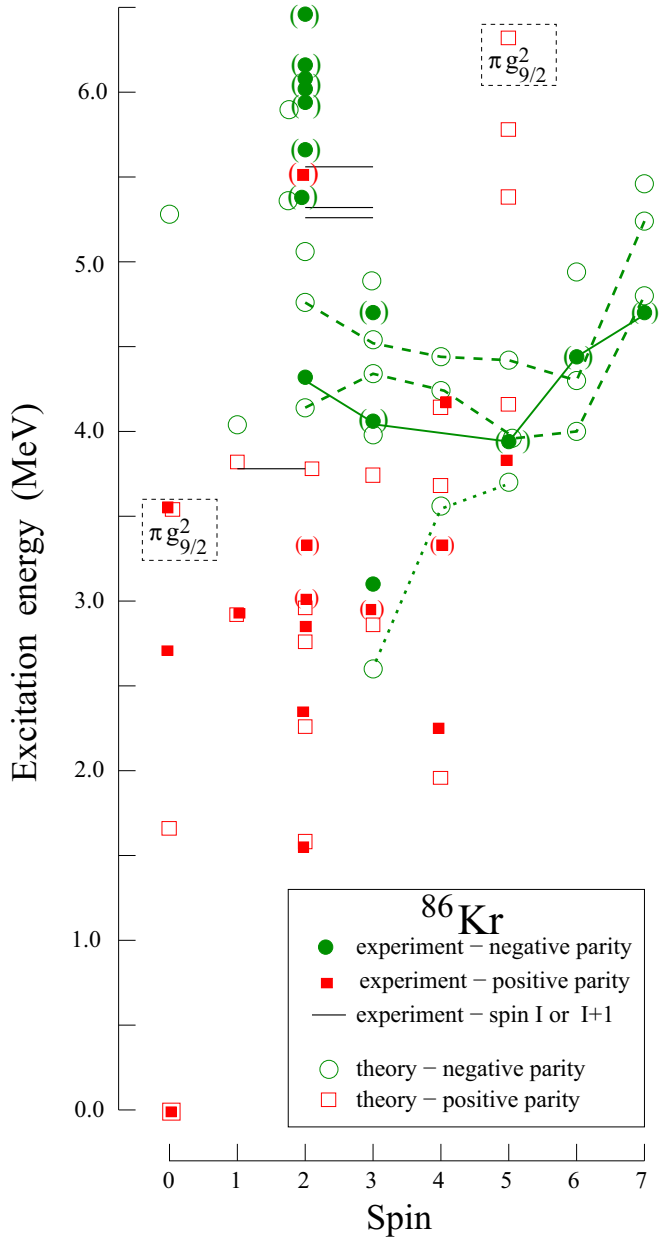

FIG. 15. Comparison of calculated and experimental levels in ^{86}Kr. Calculations are normalized to the experiment at the ground-state level. See text for more comments. The 0^+_2, 0^+_3, 4^+_2, 4^+_3, and 5^+_1 experimental levels are taken from Ref. [9].

1. ^{86}Br

In ^{86}Br the calculations reproduce exceptionally well the low-energy configurations $(\pi p_{3/2}, \nu d_{5/2})_{1^-,\ldots,4^-}$ and $(\pi f^{-1}_{5/2}, \nu d_{5/2})_{0^-,\ldots,5^-}$ (we propose for the 569.8-keV level a tentative spin and parity 1^- and for the 785.6-keV level spin and parity 0^-). When the calculations are normalized to the experiment at the 4^-_2 level, the 10 members of the multiplets, shown in Fig. 16, are reproduced with an average accuracy of 53 keV (this is the mean modulus of the difference; the mean square difference is 59 keV).

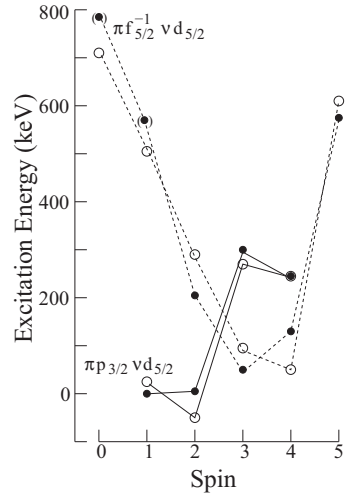

Level	Configuration $\pi p_{3/2}\,\nu d_{5/2}$	Configuration $\pi f^{-1}_{5/2}\,\nu d_{5/2}$
0_1	–	67 %
1_1	74 %	–
1_2	8 %	54 %
2_1	66 %	–
2_2	5 %	65 %
3_1	37 %	28 %
3_2	41 %	34 %
4_1	–	61 %
4_2	84 %	–
5_1	–	67 %

FIG. 16. Comparison of experimental and calculated multiplets in ^{86}Br, $(\pi p_{3/2}, \nu d_{5/2})_{1^-,\ldots,4^-}$ (connected by solid lines) and $(\pi f^{-1}_{5/2}, \nu d_{5/2})_{0^-,\ldots,5^-}$ (connected by dashed lines). Filled circles represent experimental levels and empty circles represent calculations. The "–" symbol in the table means that the contribution is lower than 5%.

The table in Fig. 16 shows the contribution (in %) of the two configurations to individual levels. We note the opposite trend in the excitation energy vs spin for the particle-particle and hole-particle configurations. It is clear that the shell model does not support spin and parity 0^- for the ground state. In the calculations the 0^- level appears around 0.75 MeV above the ground state, independent of the fine-tuning of the effective interaction.

It is worth noting that our calculations did not show any indication of a spin trap level that could suggest a beta-decaying isomer in ^{86}Br. Unless the appearance of an intruder or extruder orbital, somewhat unexpected at the $N = 50$ closed shell, this conclusion adds to the experimental refutation of the 4.5-s isomer in ^{86}Br reported before [11,12].

The calculated members of the characteristic $(\pi g_{9/2}, \nu d_{5/2})_{2^+,\ldots,7^+}$ configuration proposed in ^{86}Br [1] are linked by the dashed line in Fig. 14. In addition to the 7^+ member of the multiplet [1] there are experimental candidates for the 2^+ and 3^+ members, located close to the calculated counterparts. The contribution of the $(\pi g_{9/2}, \nu d_{5/2})_j$ configuration in wave functions of the calculated 2^+_1, 3^+_1, 4^+_1, 5^+_1, 6^+_1, and 7^+_1 levels is 80%, 72%, 80%, 74%, 73%, and 78%, respectively. The corresponding occupation numbers of the neutron and proton orbitals, as obtained in the model, are shown in Table VII. The second and the third calculated states of positive parity have significant population of the $p_{3/2}$ or $f^{-1}_{5/2}$ protons, which together with the increased population of the $h_{11/2}$ neutron orbit create the $(\pi p_{3/2}, \nu h_{11/2})_j$ and $(\pi f^{-}_{5/2}1, \nu h_{11/2})_j$ configurations with spin j, ranging from 4^+ to 7^+ and from 3^+ to 8^+, respectively. Members of these multiplets, which can be traced in Table VII, are seen in Fig. 14 between 2 and 3 MeV of excitations. It is of interest to identify experimentally these configurations, which would provide information on the excitation energy of the $h_{11/2}$ neutron at $N = 51$.

TABLE VII. Occupation of neutron and proton orbitals calculated in this work for the $(\pi g_{9/2}, \nu d_{5/2})_{2^+,\ldots,7^+}$ and $(\pi p_{3/2}, \nu h_{11/2})_{4^+,\ldots,7^+}$ multiplets in ^{86}Br. Essential numbers are shown in bold and discussed in the text. The lowest row shows occupations in the ground state of ^{86}Se.

Level	Neutron occupation					Proton occupation			
	$d_{5/2}$	$s_{1/2}$	$g_{7/2}$	$d_{3/2}$	$h_{11/2}$	$f_{5/2}$	$p_{3/2}$	$p_{1/2}$	$g_{9/2}$
2_1^+	**0.96**	0.01	0.01	0.02	0.01	5.05	0.71	0.13	**1.11**
3_1^+	**0.83**	0.01	0.01	0.13	0.01	5.06	0.71	0.11	**1.11**
3_2^+	0.77	0.07	0.01	0.14	0.02	4.33	1.40	0.20	**1.06**
4_1^+	**0.93**	0.01	0.01	0.03	0.03	5.24	0.59	0.08	**1.09**
4_2^+	0.74	0.01	0.01	0.02	**0.22**	4.56	**1.39**	0.16	0.89
5_1^+	**0.85**	0.07	0.01	0.03	0.04	4.82	0.92	0.16	**1.08**
5_2^+	0.81	0.02	0.01	0.01	0.14	4.55	1.23	0.25	0.97
5_3^+	0.69	0.08	0.01	0.02	**0.19**	4.42	**1.49**	0.17	0.92
6_1^+	**0.83**	0.01	0.01	0.01	0.13	4.95	1.00	0.08	**0.97**
6_2^+	0.77	0.01	0.01	0.02	**0.19**	4.64	**1.23**	0.15	0.98
7_1^+	**0.91**	0.01	0.01	0.01	0.08	5.28	0.58	0.10	**1.04**
7_2^+	0.85	0.02	0.01	0.02	0.10	4.21	1.58	0.10	1.01
7_3^+	0.68	0.02	0.01	0.02	**0.28**	4.67	**1.33**	0.15	0.85
1_1^+	**0.92**	0.01	0.02	0.04	0.01	4.35	**1.37**	0.20	**1.08**
1_2^+	**0.80**	0.02	**0.08**	0.08	0.01	4.49	**1.27**	0.15	**1.09**
1_3^+	**0.88**	0.02	**0.06**	0.03	0.01	4.35	**1.37**	0.18	**1.09**
1_4^+	**0.94**	0.01	0.01	0.03	0.02	4.46	**1.30**	0.15	**1.09**
1_5^+	0.38	0.03	**0.52**	0.06	0.02	4.68	1.09	0.14	**1.09**
8_1^+	**0.83**	0.01	0.01	0.01	**0.15**	4.60	**1.30**	0.17	**0.94**
^{86}Se									
0_1^+	**1.54**	0.17	**0.08**	0.13	0.08	**3.87**	1.58	0.31	0.25

In Table VII we also show calculated occupations for 1^+ levels. The 1_2^+ level is dominated (70%) by the $[\pi(f_{5/2}^{-1}, p_{3/2}, g_{9/2}), \nu d_{5/2}]$ configuration. However, it has also a distinct, 8% occupation of the neutron $g_{7/2}$ orbital, which makes it a good counterpart for the experimental 1^+ level at 2447.0 keV with $\log ft = 4.4$. The 1_3^+ level, which has 6% of the $g_{7/2}$ neutron might correspond to the 2665.4-keV level. We note that the ground state of ^{86}Se, with the dominating $\nu d_{5/2}^2$ component, has also an 8% occupation of the $g_{7/2}$ neutron orbital, as shown at the bottom of Table VII. This is analogous to the 9% admixture of the $g_{7/2}^2$ neutron, reported in the ground state of ^{92}Zr [44], the $N = 52$ isotone of ^{86}Se. These occupations fit the scenario shown in Fig. 12.

As discussed in Ref. [13], an admixture of the order of 10% of the $g_{7/2}$ neutron in the wave function of the ground state of ^{92}Kr might be sufficient to account for the $\log ft = 4.8$ of the 1^+, 1360.9-keV level in ^{92}Rb. Therefore, we have computed the $B(GT)$ values for the ^{86}Se β decay in our framework. In the present shell-model valence space, in which proton and neutron subspaces do not contain the same orbits, the $\nu g_{7/2} \rightarrow \pi g_{9/2}$ is the only possible G-T transition. This seems to be too restrictive to describe properly the allowed β decay of nuclei around $N = 50$ and our calculation predicts somewhat high $\log(ft)$ of 5.5 and 5.8 for the 1_2^+ and 1_3^+ states, respectively. Given that neither pure $\nu g_{7/2} \rightarrow \pi g_{9/2}$ nor $\nu p_{1/2} \rightarrow \pi p_{3/2}$ decays reproduce the experiment, it is advisable to mix both possibilities in the theoretical framework. Such shell-model calculations, currently not available, are planned in the future.

Strong decays of the 1^+ level at 2447.0 keV to the 2_1^-, 2_2^-, and 2_3^- levels, which have the $(\pi p_{3/2}, \nu d_{5/2})$, $(\pi f_{5/2}^{-1}, \nu d_{5/2})$, and $[\pi(p_{3/2}, f_{5/2}^{-1}), \nu d_{5/2})]$ dominating configurations, respectively, can be understood as from $E1$ transitions enhanced by octupole coupling between the $g_{9/2}$ and $p_{3/2}$ or $f_{5/2}^{-1}$ protons, present in the initial and final states, respectively.

In Ref. [15] additional distinction was introduced between the decays of 1_1^+ and 1_2^+ levels in ^{88,90,92}Rb. In ^{86}Br the 1^+, 2447.0- and 2665.4-keV levels have also different decay patterns. For example, the 2447.0-keV level decays to the 2_2^- level at 207.0 keV while the other level does not. The reason could be the occupation of the $f_{5/2}^{-1}$ proton hole, present in the 2_2^- level, as seen Fig. 16. The contribution of the $[\pi(p_{3/2}, f_{5/2}^{-1}), \nu d_{5/2})]$ configuration in the 1_2^+ calculated level is higher (45%) than in the 1_3^+ level (30%).

The 1_5^+ level, shown in a dashed-line box in Fig. 14 might be a good source of information on the $\pi g_{9/2}$ and $\nu g_{7/2}$ orbitals, provided its experimental counterpart is identified. The level predicted at 3.1 MeV is dominated (43%) by the $(\pi g_{9/2}, \nu g_{7/2})$ configuration. We note, though, that no super population of this level is expected in β decay of the ground state of ^{86}Se, where the admixture of the $g_{7/2}$ neutron is 8% only.

Finally, the theoretical counterpart for the 8^+ experimental level at 3240 keV is dominated (66%) by the $[\pi(g_{9/2}), \nu d_{5/2}]$ configuration with a 9% admixture of the $(\pi f_{5/2}^{-1}, \nu h_{11/2})$ configuration. The occupation of the $g_{7/2}$ neutron is here below 1%.

2. ^{86}Kr

The negative-parity, 2^- to 7^- levels between 4 and 5 MeV of excitation are reproduced satisfactorily as members

TABLE VIII. Occupation of proton orbitals and contributions in wave functions calculated for the $\pi(f_{5/2}^{-1}g_{9/2}^{1})$, $\pi(p_{3/2}^{1}g_{9/2}^{1})$, and $\pi(p_{3/2}^{3}g_{9/2}^{1})$ multiplets in ^{86}Kr. Only contributions larger than 5% are considered. Essential numbers are shown in bold and discussed in the text.

Level	Configuration contribution		Proton occupation			
	$\pi(f_{5/2}^{-1}g_{9/2}^{1})$	$\pi(p_{3/2}^{1}g_{9/2}^{1})$ $+\pi(p_{3/2}^{3}g_{9/2}^{1})$	$f_{5/2}$	$p_{3/2}$	$p_{1/2}$	$g_{9/2}$
2_1^-	**50%**	<5% + 31%	4.51	2.23	0.15	1.10
2_2^-	**58%**	<5% + 9%	4.66	1.90	0.27	1.17
2_3^-	39%	<5% + 33%	4.27	2.35	0.21	1.16
3_1^-	6%	**70%** + 12%	5.46	1.32	0.06	1.16
3_2^-	22%	17% + **41%**	4.51	2.19	0.18	1.12
3_3^-	**61%**	<5% + 19%	4.67	2.07	0.13	1.13
3_4^-	**50%**	<5% + 20%	4.59	2.03	0.25	1.14
4_1^-	23%	**56%** + 8%	5.37	1.44	0.07	1.12
4_2^-	**49%**	11% + 9%	4.84	1.76	0.28	1.12
4_3^-	**73%**	<5% + 9%	4.76	1.99	0.12	1.13
5_1^-	23%	**56%** + 6%	5.40	1.38	0.08	1.14
5_2^-	**47%**	9% + 22%	4.64	2.02	0.17	1.17
5_3^-	**67%**	8% + <5%	4.86	1.86	0.15	1.12
6_1^-	**57%**	18% + 7%	4.88	1.87	0.13	1.12
6_2^-	**63%**	11% + 10%	4.87	1.87	0.11	1.15
6_3^-	33%	39% + 7%	5.18	1.52	0.16	1.14
7_1^-	**68%**	<5% + 10%	4.62	2.09	0.15	1.14
7_2^-	**58%**	<5% + 20%	4.53	2.17	0.16	1.14
7_3^-	39%	<5% + 31%	4.41	2.23	0.25	1.11

of the $\pi(f_{5/2}^{-1},g_{9/2})_{2^-,\ldots,7^-}$ multiplet, expected here. This configuration is mixed with two other configurations, $\pi(p_{3/2}^{1},g_{9/2})$ and $\pi(p_{3/2}^{3},g_{9/2})$.

Table VIII shows occupations of proton orbitals and contributions of the three dominating configurations to wave functions of the calculated 2^- to 7^- levels. The $2_{1,2}^-$, $3_{3,4}^-$, $4_{2,3}^-$, $5_{2,3}^-$, $6_{1,2}^-$, and $7_{1,2}^-$ levels are dominated by the $\pi(f_{5/2}^{-1},g_{9/2})$ configuration and show the energy vs spin dependence characteristic of the hole-particle coupling (linked by dashed lines in Fig. 15). Such dependence is also seen for the experimental members of the multiplet (linked by solid line). Thus the present calculations strongly support the newly proposed interpretation of the 4316.1-keV level in ^{86}Kr as the $\pi(f_{5/2}^{-1},g_{9/2})_{2^-}$ structure populated in the G-T decay of the $g_{7/2}$ neutron, admixed in the ground state of ^{86}Br.

The structure of the 3_1^- 4_1^- and 5_1^- calculated levels is dominated by the $\pi(p_{3/2},g_{9/2})$ configuration (linked by dotted line in Fig. 15). The 3_1^- level appears 500 keV lower than its possible experimental counterpart. This level (or any other negative-parity level) was not included in our fit of the proton-proton interaction for the even-even $N = 50$ nuclei performed in Ref. [5]. It would be of interest to identify experimentally other members of this multiplet for further refinements of the shell-model Hamiltonian.

3. ^{86}Kr 1^+ *level*

The 1_1^+ excitation in ^{86}Kr is a new phenomenon observed at $N = 50$. This level together with the nearby 2^+ levels and the 3_1^+ level resemble the pattern of the so-called mixed-symmetry states identified at $N = 52$ in ^{94}Mo [45]. However, such a pattern is unexpected in ^{86}Kr because at $N = 50$ there are no valence neutrons to produce mixed-symmetry states.

Figure 17(a), showing the 1_1^+ level and associated levels in ^{86}Kr, should be compared to Fig. 1 of Ref. [46] showing the mixed-symmetry pattern in ^{94}Mo at $N = 52$. There are similarities, but also clear differences. In ^{86}Kr one does not expect the two-phonon, symmetric excitations 0_1^+, 2_2^+, and 4_1^+. Instead, the 2_2^+, 2349.6-keV level of ^{86}Kr is an analog of the 2_3^+, Q_m mixed-symmetry state of ^{94}Mo and the 4_1^+ level behaves like 2_2^+. The 1_1^+, 2_3^+, and 3_1^+ levels in ^{86}Kr, seen about $\Delta E = E(4_1^+) - E(2_1^+)$ above the 2_2^+ level, are analogous to the $Q_m Q_s$ multiplet of ^{94}Mo. We also note the small mixing ratios of the 501.4- and 785.0-keV transitions and pronounced

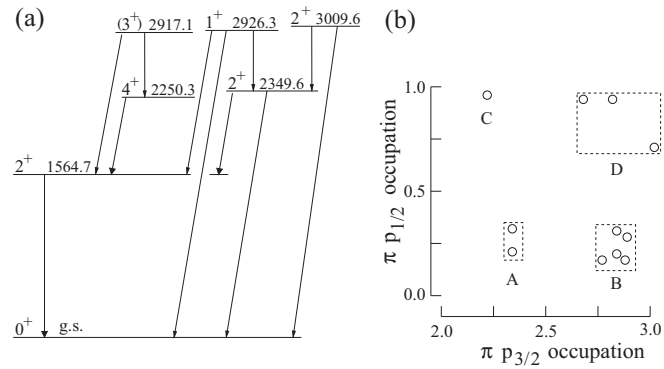

FIG. 17. (a) Partial scheme of low-spin excitation in ^{86}Kr drawn to assist the discussion. (b) Occupation of $\pi p_{3/2}$ vs $\pi p_{1/2}$ orbitals for the levels of ^{86}Kr, shown at the left-hand side. See text for the meaning of the A, B, C, and D labels.

TABLE IX. $B(M1)$ values obtained in the present shell-model framework for selected transitions in ^{86}Kr.

$J_f^\pi \rightarrow J_i^\pi$	$B(M1)$ (μ_N^2)
$2_2^+ \rightarrow 2_1^+$	0.25
$2_3^+ \rightarrow 2_2^+$	0.11
$3_1^+ \rightarrow 4_1^+$	0.17
$1_1^+ \rightarrow 2_2^+$	0.14
$1_1^+ \rightarrow 2_3^+$	0.17

decay branches in ^{86}Kr from the 1_1^+, 2_3^+, and 3_1^+ levels to the 2_1^+, 2_2^+, and 4_1^+ levels, analogous to $M1$ transitions in ^{94}Mo.

This analogy is supported by the present shell-model calculations. In Table IX we list the strongest $M1$ transitions between the levels depicted in Fig. 17(a). The 2_2^+ level has a strong $M1$ branch to the 2_1^+ level, while the calculated $B(E2; 2_2^+ \rightarrow 0^+) = 18e^2\,\mathrm{fm}^4$ is small, which is a characteristic feature of a mixed-symmetry state in a nucleus with valence proton-neutron excitations. Also, the 3^+ level has the strongest $M1$ transition to the 4^+, replacing in this scheme the 2_2^+ of ^{94}Mo.

In ^{86}Kr these $M1$ decays are from the structure of the wave functions, as shown in Table X, where the levels are grouped according to their proton occupations (groups A, B, C, D). The dominating modes of excitations correspond here to the promotion of protons from the $f_{5/2}$ orbital to the $p_{3/2}$ and $p_{1/2}$ orbitals, favoring $M1$ transitions. This is illustrated in Fig. 17(b). The levels 0_1^+ and 2_1^+ (group A) have similar occupations ("initial"). The levels 1_1^+, 2_2^+, 3_1^+, and 4_1^+ (group B) correspond to the increased occupation of the $p_{3/2}$ orbital while the 1_2^+ level (C), has an increased occupation of the $p_{1/2}$ orbital. The 2_3^+ and 3_2^+ levels (group D) have increased occupation of both $p_{1/2}$ and $p_{3/2}$ orbitals. The decays shown in Fig. 17(a) correspond to transitions between $f_{5/2}$ and $p_{3/2}$ protons [B $\rightarrow$ A in Fig. 17(b)].

TABLE X. Occupation of proton orbitals in selected levels of ^{86}Kr. See the text for more comments.

Level	Group	Proton occupation			
		$f_{5/2}$	$p_{3/2}$	$p_{1/2}$	$g_{9/2}$
0_1^+	A	5.06	2.34	0.21	0.40
2_1^+	A	5.06	2.34	0.32	0.28
1_1^+	B	4.79	2.78	0.17	0.26
2_2^+	B	4.60	2.89	0.28	0.24
2_4^+	B	4.60	2.86	0.30	0.25
3_1^+	B	4.72	2.84	0.20	0.24
4_1^+	B	4.69	2.87	0.17	0.27
1_2^+	C	4.57	2.22	0.96	0.24
2_3^+	D	4.00	2.82	0.94	0.24
3_2^+	D	4.03	2.72	1.04	0.21
4_3^+	D	4.15	2.67	0.94	0.25
0_2^+		4.52	3.03	0.20	0.25
4_2^+		3.99	3.34	0.44	0.23
0_3^+		5.33	0.71	0.22	1.74
5_4^+		4.69	1.22	0.06	2.04

It is an intriguing question if the similarity of the discussed patterns in ^{86}Kr and ^{94}Mo is accidental or whether there is some relation between them. We note that in ^{92}Zr where, similarly as in ^{86}Kr, the 0_2^+, 2_2^+, and 4_1^+, two-phonon states are not expected [46], the 2_2^+ level is proposed as a mixed-symmetry state [46]. In the shell-model calculations of "mixed-symmetry" states in ^{94}Mo [47], the 1_1^+, 2_3^+, and 3_2^+ were found to show common proton-neutron symmetry on the microscopic level. On the other hand, no experimental candidates for the 0^+ and 4^+ mixed-symmetry states are identified in ^{94}Mo [46,48,50] (a candidate for the 4^+ m.s. state is proposed at 2564.9 keV). Furthermore, at $N > 52$ the mixed-symmetry pattern is less evident [46,49].

This suggests a picture, where a "basic" proton structure formed at $N = 50$ (primarily, the $\pi(f_{5/2}^{-1}, p_{3/2})_{1^+,2^+,3^+,4^+}$ configuration), is enriched at $N = 52$ by excitations from the two valence neutrons (the 2_1^+ in ^{92}Zr is calculated as a neutron excitation [46]), showing proton-neutron coupling, though not sufficient to generate the 0^+ and 4^+ "mixed-symmetry" states. At $N > 52$ this structure is fragmented [49], probably because of further neutron excitations and the emerging collectivity, diffusing the mixed-symmetry pattern.

4. ^{86}Kr *other observations.*

The 0_3^+ and 5_4^+ calculated levels (inside dashed-line boxes in Fig. 15) are nearly pure $\pi g_{9/2}^2$ configurations (see Table X). It is of interest to investigate the structure of the 0_3^+ experimental level [9] and to search for the experimental counterpart of the 5_4^+ level as both levels could provide energy of the $g_{9/2}$ proton orbital at $Z = 36$.

The only large deviation between the calculated, positive-parity levels and the experiment is observed for the 0_2^+ level. The theoretical 0_2^+ level, calculated at a somewhat low energy of 1.6 MeV, is from the excitation of the $f_{5/2}$ proton to the $p_{3/2}$ orbital. In view of such a distinct prediction, it is important to search for a possible, new experimental counterpart of the 0_2^+ calculated level.

IV. SUMMARY

Properties of ^{86}Br and ^{86}Kr, populated in β^- decay have been reinvestigated. Inconsistencies existing in the literature were removed and a new scenario for the Gamow-Teller β^- decays of ^{86}Se and ^{86}Br was proposed.

New levels and transitions found in ^{86}Br show that the population of the 53.1-keV level in ^{86}Br in β^- decay of ^{86}Se is negligible, confirming its 3^- spin and parity. The spin and parity of the ground state of ^{86}Br is firmly established to be 1^- and we reject the existence of a hypothetical 5-s, β-decaying isomer in ^{86}Br.

Measurements and novel calculations of directional-linear-polarization correlations allowed the unique, $I^\pi = 2^-$ spin and parity assignment to the 4316.1-keV level in ^{86}Kr. We propose that this level belongs to the $(\nu f_{5/2}^{-1}, \pi g_{9/2})$ multiplet and its strong population in β decay of the 1^- ground state of ^{86}Br is from an admixture of the $\nu g_{7/2} \rightarrow \pi g_{9/2}$ G-T transition.

In ^{86}Kr, at 3 MeV of excitation we identified 1_1^+, 2_2^+, and 3_1^+ levels analogous to the mixed-symmetry states in ^{94}Mo. In ^{86}Kr

these states are from proton excitations only, raising questions about the microscopic origin of mixed-symmetry states near closed shells.

The experimental results are supported by the large-scale, shell-model calculations performed in this work, using refined interactions. In ^{86}Br all members of the $(\pi f_{5/2}^{-1}, \nu d_{5/2})$ and $(\pi p_{3/2}, \nu d_{5/2})$ multiplets are very well reproduced in the calculations. Importantly, for the 1^+, 2447.0-keV level in ^{86}Br, the calculated counterpart has an 8% contribution of the $g_{7/2}$ neutron, supporting the proposed scenario for the G-T decay. This picture is further confirmed by a successful reproduction of the $\pi(f_{5/2}^{-1}, g_{9/2})$ multiplet in ^{86}Kr. Worth noting is that the calculations predict also the $\pi(p_{3/2}, g_{9/2})$ multiplet in ^{86}Kr, for which there are three experimental candidates.

It is important to confirm the proposed interpretations. First of all, one should identify missing members of the $\pi(f_{5/2}^{-1}, g_{9/2})$ and $\pi(p_{3/2}, g_{9/2})$ multiplets in ^{86}Kr and confirm the 0^- and 1^- spin assignments proposed for the 569.8- and 785.6-keV levels in ^{86}Br.

ACKNOWLEDGMENTS

The authors acknowledge discussions with Professor A. Płochocki. This work was supported by the Polish National Science Centre under Contract No. DEC-2013/09/B/ST2/03485. The authors thank the technical services of the ILL, LPSC, and GANIL for supporting the EXILL campaign. The EXOGAM collaboration and the INFN Legnaro are acknowledged for the loan of Ge detectors.

[1] M.-G. Porquet, A. Asteir, Ts. Venkova, I. Deloncle, F. Azaiez, A. Buta, D. Curien, O. Dorvaux, G. Duchêne, B. J. P. Gall *et al.*, Eur. Phys. J. A **40**, 131 (2009).
[2] K. Sieja, T. R. Rodriguez, K. Kolos, and D. Verney, Phys. Rev. C **88**, 034327 (2013).
[3] T. Rząca-Urban, M. Czerwiński, W. Urban, A. G. Smith, I. Ahmad, F. Nowacki, and K. Sieja, Phys. Rev. C **88**, 034302 (2013).
[4] M. Czerwiński, T. Rząca-Urban, K. Sieja, H. Sliwinska, W. Urban, A. G. Smith, J. F. Smith, G. S. Simpson, I. Ahmad, J. P. Greene, and T. Materna, Phys. Rev. C **88**, 044314 (2013).
[5] M. Czerwiński, T. Rząca-Urban, W. Urban, P. Bączyk, K. Sieja, B. M. Nyakó, J. Timar, I. Kuti, T. Tornyi, L. Atanasova, A. Blanc, M. Jentschel, P. Mutti, U. Köster, T. Soldner, G. de France, G. Simpson, and C. A. Ur, Phys. Rev. C **92**, 014328 (2015).
[6] M. Czerwiński, T. Rząca-Urban, W. Urban, P. Bączyk, K. Sieja, J. Timar, I. Kuti, T. Tornyi, B. Nyakó, L. Atanasova, A. Blanc, M. Jentschel, P. Mutti, U. Köster, T. Soldner, G. de France, G. Simpson, and C. A. Ur, Phys. Rev. C **93**, 034318 (2016).
[7] T. Materna, W. Urban, K. Sieja, U. Köster, H. Faust, M. Czerwiński, T. Rząca-Urban, C. Bernards, C. Fransen, J. Jolie, J.-M. Regis, T. Thomas, and N. Warr, Phys. Rev. C **92**, 034305 (2015).
[8] J. Litzinger, A. Blazhev, A. Dewald, F. Didierjean, G. Duchêne, C. Fransen, R. Lozeva, K. Sieja, D. Verney, G. de Angelis, D. Bazzacco *et al.*, Phys. Rev. C **92**, 064322 (2015).
[9] A. Negret and B. Singh, Nucl. Data Sheets **124**, 1 (2015).
[10] M. Zendel, N. Trautmann, and G. Herrmann, J. Inorg. Nucl. Chem. **42**, 1387 (1980).
[11] A. Lundán, Z. Phys. **236**, 403 (1970).
[12] T. R. England and B. F. Rider, *Fission Product Yields per 100 Fissions for ^{235}U Thermal neutron Induced Fission Decay*, La-UR-94-3016, ENDF-349 (Los Alamos National Laboratory, Los Alamos, 1993).
[13] R. J. Olson, W. L. Talbert Jr., and J. R. McConnell, Phys. Rev. C **5**, 2095 (1972).
[14] R. J. Bunting, W. L. Talbert Jr., J. R. McConnell, and R. A. Meyer, Phys. Rev. C **13**, 1577 (1976).
[15] C. L. Duke, W. L. Talbert Jr., F. K. Wohn, J. K. Halbig, and K. B. Nielsen, Phys. Rev. C **19**, 2322 (1979).
[16] Y. Funakoshi, K. Okano, and Y. Kawase, Nucl. Phys. A **431**, 461 (1984).
[17] G. Lhersonneau, S. Brant, H. Ohm, V. Paar, K. Systemich, and D. Weiler, Z. Phys. A **334**, 259 (1989).
[18] C. Mazzocchi, K. P. Rykaczewski, R. Grzywacz, P. Bączyk, C. R. Bingham, N. T. Brewster, C. J. Gross, C. Jost, M. Karny, A. Korgul, M. Madurga, A. J. Mendez II, K. Miernik *et al.*, Phys. Rev. C **92**, 054317 (2015).
[19] P. Armbruster *et al.*, Nucl. Instr. Meth. **139**, 213 (1976).
[20] G. Fioni, H. R. Faust, M. Gross, M. Hesse, P. Armbruster, F. Gönnenwein, and G. Münzenberg, Nucl. Instr. Meth. A **332**, 175 (1993).
[21] The Joint Evaluated Fission and Fusion File (JEFF) [http://www.oecd-nea.org/dbdata/jeff/].
[22] P. Mutti *et al.*, EPJ Web Conferences **62**, 01001 (2013).
[23] M. Jentschel *et al.* (unpublished).
[24] H. Abele *et al.*, Nucl. Instr. and Meth. A **562**, 407 (2006).
[25] J. Simpson, F. Azaiez, G. deFrance, J. Fouan, J. Gerl, R. Julin, W. Korten, P. J. Nolan, B. M. Nyakó *et al.*, APH N. S., Heavy Ion Physics **11**, 159 (2000).
[26] I. Ahmad and W. R. Phillips, Rep. Prog. Phys. **58**, 1415 (1995).
[27] W. B. Walters, E. A. Henry, and R. A. Meyer, Phys. Rev. C **29**, 991 (1984).
[28] J. Lin, K. Rengan, and R. A. Meyer, Radiochem. Radioanal. Lett. **50**, 399 (1982).
[29] "Tools and Publications" service, [http://www.nndc.bnl.gov].
[30] M. H. Hurdus and L. Tomlinson, J. Inorg. Chem. **37**, 1 (1975).
[31] N. Fotiades, M. Devlin, R. O. Nelson, and T. Granier, Phys. Rev. C **87**, 044336 (2013).
[32] G. Winter, R. Schwengner, J. Reif, H. Prade, L. Funke, R. Wirowski, N. Nicolay, A. Dewald, P. von Brentano, H. Grawe, and R. Schubart, Phys. Rev. C **48**, 1010 (1993).
[33] A. Prévost. M. G. Porquet, A. Astier, I. Deloncle, F. Azaiez, A. Buta, D. Curien, O. Dorvaux, G. Duchêne, B. J. P. Gall *et al.*, Eur. Phys. J. A **22**, 391 (2004).
[34] P. M. Jones, L. Wei, F. A. Beck, P. A. Butler, T. Byrski, G. Duchêne, G. De France, F. Hannachi, G. D. Jones, and B. Kharraja, Nucl. Data Sheets **113**, 2187 (2012).
[35] P. J. Nolan, F. A. Beck, and D. B. Fossan, Ann. Rev. Nuc. Part. Sci. **44**, 561 (1994).

[36] K. S. Krane, R. M. Steffen, and R. M. Wheeler, Nucl. Data Tables **11**, 351 (1973).
[37] W. D. Hamilton, ed., *The Electromagnetic Interaction in Nuclear Spectroscopy* (North-Holland Publishing, Amsterdam 1975).
[38] T. Aoki, K. Furuno, Y. Tagishi, A. Ohya, and J.-Z. Ruan, At. Data Nucl. Data Tables **23**, 349 (1979).
[39] W. Urban, M. Jentschel, B. Märkisch, Th. Materna, Ch. Bernards, C. Drescher, Ch. Fransen, J. Jolie, U. Köster, P. Mutti, T. Rząca-Urban, and G. S. Simpson, JINST **8**, P03014 (2013).
[40] W. Urban, K. Sieja, G. S. Simpson, T. Soldner, T. Rząca-Urban, A. Złomaniec, I. Tsekhanovich, J. A. Dare, A. G. Smith, J. L. Durell, J. F. Smith, R. Orlandi, A. Scherillo, I. Ahmad, J. P. Greene, J. Jolie, and A. Linneman, Phys. Rev. C **85**, 014329 (2012).
[41] I. Tsekhanovich, G. S. Simpson, W. Urban, J. A. Dare, J. Jolie, A. Linnemann, R. Orlandi, A. Scherillo, A. G. Smith, T. Soldner, B. J. Varley, T. Rząca-Urban, A. Złomaniec, O. Dorvaux, B. J. P. Gall, B. Roux, and J. F. Smith, Phys. Rev. C **78**, 011301(R) (2008).
[42] K. Sieja, F. Nowacki, K. Langanke, and G. Martínez-Pinedo, Phys. Rev. C **79**, 064310 (2009).
[43] E. Caurier, G. Martinez-Pinedo, F. Nowacki, A. Poves, and A. P. Zuker, Rev. Mod. Phys. **77**, 427 (2005).
[44] J. B. Ball and C. B. Fulmer, Phys. Rev. **172**, 1199 (1968).
[45] N. Pietralla, C. Fransen, D. Belic, P. von Brentano, C. Friessner, U. Kneissl, A. Linnemann, A. Nord, H. H. Pitz, T. Otsuka, I. Schneider, V. Werner, and I. Wiedenhoeven, Phys. Rev. Lett. **83**, 1303 (1999).
[46] S. W. Yates, J. Radioanal. Nucl. Chem. **265**, 291 (2005).
[47] A. F. Lisetskiy, N. Pietralla, C. Fransen, R. V. Jolos, and P. von Brentano, Nucl. Phys. A **677**, 100 (2000).
[48] C. Fransen, N. Pietralla, Z. Ammar, D. Bandyopadhyay, N. Boukharouba, P. von Brentano, A. Dewald, J. Gableske, A. Gade, J. Jolie, U. Kneissl, S. R. Lesher, A. F. Lisetskiy, M. T. McEllistrem, M. Merrick, H. H. Pitz, N. Warr, V. Werner, and S. W. Yates, Phys. Rev. C **67**, 024307 (2003).
[49] T. Thomas, V. Werner, J. Jolie, K. Nomura. T. Ahn, N. Cooper, H. Duckwitz, A. Fitzler, C. Fransen, A. Gade, M. Hinton, G. Ilie, J. Jenssen, A. Linnemann, P. Petkov, N. Pietralla, and D. Radeck, Nucl. Phys. A **947**, 203 (2016).
[50] V. Werner, D. Belic, P. von Brentano, C. Fransen, A. Gade, H. von Garrel, J. Jolie, U. Kneissl, C. Kohstall, A. Linnemann, A. F. Lisetskiy, N. Pietralla, H. H. Pitz, M. Sheck, K.-H. Speidel, F. Stedile, and S. W. Yates, Phys. Lett. B **550**, 140 (2002).